MECHANICAL OPTIMIZATION OF CERAMIC-BASED COMPOSITES FOR WATER FILTRATION

ASHESI UNIVERSITY

CAPSTONE PROJECT

B.Sc. Mechanical Engineering

Augustus Poku Sarkodee (ID: 35902021)

MAY 2021

ASHESI UNIVERSITY

MECHANICAL OPTIMIZATION OF CERAMIC-BASED COMPOSITES FOR WATER FILTRATION

CAPSTONE PROJECT

Capstone Project submitted to the Department of Engineering, Ashesi University in partial fulfilment of the requirements for the award of Bachelor of Science degree in Mechanical Engineering.

Augustus Poku Sarkodee

2021

DECLARATION

I hereby declare that this capstone is the result of my own original work and that no part of it has been presented for another degree in this university or elsewhere.

Candidate's Signature:

……**A.P.S**……

Candidate's Name:

……Augustus Poku Sarkodee……

Date:

……**April 27, 2021**……

I hereby declare that the preparation and presentation of this capstone were supervised in accordance with the guidelines on the supervision of capstone laid down by Ashesi University.

Supervisor's Signature:

……

Supervisor's Name:

……

Date:

……

Acknowledgements

To the Almighty Lord for granting my strength, good health and mental stability to complete this project.

To my supervisor, Dr. Danyuo Yiporo for his patience and guidance through this topic and enabling me to understand all the nuances of this project

To my parents for the ability to create a conducive environment that enabled me to work from home to the best of my ability

ABSTRACT

The production of ceramic filters is one that many organizations and individuals have undertaken to curb the spread of waterborne diseases and ailments arising from harmful microorganisms and the mishandling of water bodies. These ceramic filters often have a lifespan of close to 2 years, and on occasion, even shorter time due to mishandling of the filters or their ability to perform to full functionality over a short period. This paper seeks to tackle the issue of many of these filters not being mechanically optimized, causing either early structural damage or insufficient flowrate. Doing this required analysis to find both the right taper angle and height configurations of the filter, as well as the best composite ratio of clay and combustible material, in which the porosity level is large enough for a sufficient flowrate while ensuring that it of good strength. Simulations provided on stress and strain analysis done in SolidWorks show that taper angles of 10^{o} with a height of 20cm and 20^{o} and a height of 30cm would be appropriate while having a clay to the combustible material ratio of 70:30 would be ideal.

Table of Contents

List of Table of Figures

List of Figures

CHAPTER ONE

1.0 Introduction

1.1 Background

Water is the foundation on which individuals thrive, societies bloom, countries grow, and the world, at large, blossoms. As such, its *potability*, in retrospect, is essential, and to many aspects, a right for every human, irrespective of who they are. Recognizing that the pillar on which we as humans find ourselves, it is essential that provision is made for every human to have access to potable drinking water, which is in line with the United Nations (UN) Sustainable Development Goal 6 (Clean Water and Sanitation).

Essentially, every human being deserves portable drinking water, irrespective of their respective backgrounds. As such, it is the responsibility of global governing health organizations, such as the World Health Organization (WHO), to determine the conditions necessary to determine the necessary criteria under which water will be classified as being safe for consumption and usage. 80% of the world's wastewater going untreated and stemming from natural activities like floods and human activities such as mining, toxic industrial exchanges down to human waste [1]. Reports from research undertaken by a team at the Borgen Project suggest that the number one cause of pollution in major water bodies within Ghana has been rapid urbanization [2]. Urbanization requires mass building and scaling of environments to make them more 'habitable' to a modernized society's standard, and this rarely considers the negative externalities borne out of it. To appropriately understand the extent of this externality, WaterAid US reports suggest that a fifth of the total Ghanaian population does not have access to clean water [3]. This data approximates that 6 million Ghanaians live without the basic right to clean, potable water.

A variety of ailments have arisen due to water pollution, with one of the most active being early childhood diarrhea (ECD). 60% of global diarrhea-related deaths have been caused by unsanitary water, and more than 22 % of these deaths occurring within Sub-Saharan Africa [4], with close to 485,000 diarrheal deaths each year [5]. As such, it was identified that 6,899 Ghanaian children were affected by diarrheal-related infections and fatalities in 2017 [6]. Adjei et al. [7] report that stool samples of 277 Ghanaian children infected with diarrhea contained Cryptosporidium *spp*, the primary diarrhea-causing microscopic parasite. Cryptosporidium *spp* is usually found in the feces of infected humans and animals and its main mode of infection is through ingestion, usually of water or contaminated food. This led to the understanding that many infected children or households do not have direct access to clean water, general sanitary conditions, and proper hygiene infrastructure. This is almost and always proportional to their living standards, which inadvertently can be tied to their income level.

Hence, the need for a low-cost device that affected families can begin to use for water filtration. The goal of this work is to mechanically optimize ceramic-based composites for water filtration.

1.2 Problem Statement

Cryptosporidium *spp*, along with a variety of bacteria matter such as Escherichia coli (E. Coli) (a Gram-negative coliform bacterium) have found their way into major water bodies within rural communities and urban in Ghana [7]. Many of these water bodies have several tributaries which carry wastewater into their mainstreams. As a result of harmful microorganisms and particulate pollution on surface waters, there is the need to filter and treat surface waters for riddance of these harmful microorganisms. However, in doing so, many households tend to lose access to their clean/potable water when their ceramic filters break due to mishandling or accident [29]. Optimization of clay composites for the appropriate porosity that can support flow rate as

well as offer a sustained mechanical property would be explored in this study using drop test/impact studies.

1.3 Motivation and Justification

Having acknowledged the presence of these harmful microorganisms within the water bodies of many communities, some private and institutional organizations have made attempts to either mass clean these reserves or encourage residents to take charge of their environment. There have been some successes with other forms of filtration such as plain sedimentation [8], chlorination [9], as well as aeration [10]. These methods have varying cost structures attached to them depending on the organisms needed to removed pollutants from water.

Traditionally, most communities' results to boiling contaminated/polluted waters. Whilst boiling essentially may kill bacteria and viruses in water, it causes it to settle at the bottom, rather than eliminating their presence in the water [11]. Most communities in Ghana have been polluted by illegal mining activities. Boiling will result in an increase in the concentration of heavy metals in solution. Boiling, therefore, is not a recommended approach to dealing with polluted waters in mining communities because of the use of toxic metal or chemicals used by illegal miners such as mercury (Hg), lead (Pb) [12], Arsenic (As), Copper (Cu), amongst others [13].

This work proposed the use of ceramic-vessel filtration. This is an extremely cost-effective method of filtration that makes use of locally sourced materials. This filter uses fine sand, coarse sand, and gravel to sieve and remove relatively large particles within the water incorporated at the top of the vessel, as seen in the image below. This is useful for places where the main concern is muddy and particle-ridden water. However, the presence of mud and particles is an indication of dirt, which in turn could be filled with a host of bacteria and viruses; many of which cannot be

filtered by sand and gravel (Fig. 1.1), due to their microbial sizes. However, this work proposed to use UV-Visible light to destroy bacteria in filtered water. This research is of great importance, and it ties directly in line with the 6th SDG (providing clean water and sanitation for every household).

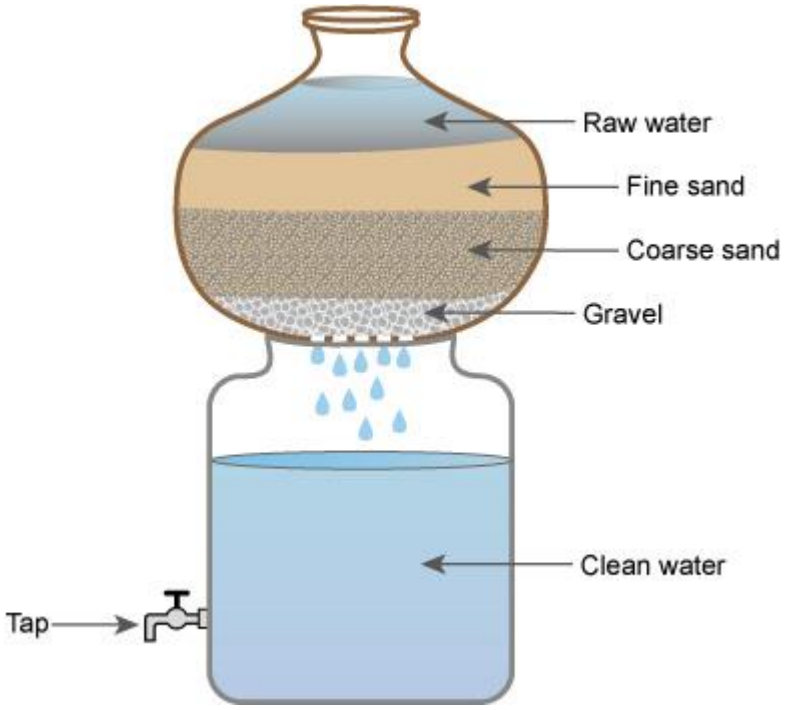

Figure 1.1: *Ceramic Filtration with Fine sand, Coarse Sand, and Coarse Sand [14]*

1.4 End Goal and Specific Objectives

Looking into the immediate future, the main goal of this research piece is to garner information for the analysis and optimization of a ceramic filter for water filtration. In my bid to do this, I would need to efficiently understand how water filtration through a ceramic filter works, which compositions of ceramic composites with reinforced sawdust are best for specific filtration purposes (chemical or physical particle filtration) and under which conditions, if any, this filter would work at its optimum performance. This would be done through the studying of ceramic water filters in the literature and hence identifying their unresolved issues for positive outcomes. Some specific objectives of this project include:

- Conceptual designs of ceramic filters for optimization: identifying the most efficient shape or angle of tapping, depth of filter, and effect of filter filler radius.
- Computational modeling and simulation of mechanical and flow properties.
- Study the effect of composite material porosity of water filter.
- Study the effect of porosity on flow rate and mechanical properties of the filter.
- Study the flowrate of the ceramic filters as a function of porosity and taped angle.

1.5 Scope of Work

Background studies and statics on water pollution and consequences of health challenges are presented in chapter one. The second chapter intends to build upon an existing knowledge of ceramic-based composite filters in a bid to optimize their mechanical properties, porosity, shapes, with a potential consequence of reducing the cost structures associated with production. Analysis would be done for filters of a variety of compositions and designs in the third chapter. Analysis done would include the study of the porosity on the flow rate and, the flowrate as a function of porosity and tapered angle. Knowledge of an improved filter design would be discussed to produce filters for communities with relatively high cases of bacteria-causing ailments and diseases within rural parts of Ghana.

CHAPTER TWO

2.0 Literature Review

2.1 Background Statistics on the Consequences of Drinking Contaminated Water

The United Nations (UN) statistics has shown that 785 million people in the World lacks access to safe drinking-water service-a basic service is essentially a drinking water source situated within a 30-minute round trip for water [15]. Developing countries suffers a lot of setbacks due to poor drinking water. Some of which a largely negative socio-economic impact on communities where people must spend a relatively large amount of time to physically collect water from far, risky, and often from unsafe places [15]. The main concern associated with the lack of clean drinking water is the obvious health challenges associated with affected communities, especially with increased cases of disease such as cholera, dysentery, diarrhea, and typhoid. These diseases are caused by bacteria and viruses usually that are found and bred in unclean water. Cholera is caused by a bacterium known as *Vibrio Cholerae,* which usually causes the spread of toxins in small intestines leading to rapid loss of bodily fluids and in most cases, diarrhea [16]. With Africa representing 54% of the 132,121 worldwide cases of cholera in the world in 2016 [17], there has been an increase in the attention towards the need to provide clean water for affected communities, mainly many of which exist in rural areas.

The availability of potable water, especially in rural, underdeveloped communities has been made increasingly accessible due to innovations in water filter technologies; many of which are produced with locally sourced materials and low-cost production methods. However, recent activities in countries like Ghana such as illegal mining, also known as *Galamsey* has increased the level of pollution within surface waters. Ampomah estimates that over 60% of pollution in

Ghana's water bodies is caused by a combination of industrial waste, illegal mining, farming, and household disposals [18].

Unfortunately, most of the polluted water bodies serve as the primary source of water for domestic use and human consumption. The current situation in the country calls for urgent attention by providing local solutions that will be beneficial both internally and externally for all affected communities. Kani and Nair [20] did some extensive research into a range of naturally sourced materials, including sand, garnet, and laterite, differing their compositions, strength, and flowrates. This project would make use of ceramic-based composites such as clay, sawdust/rice husk, and charcoal, as exhibited by Ajayi and Lamidi [20]. This production method is largely considered to be low-cost, especially within rural areas known for the abundance of clay and biomass, often considered as waste. Filter preparation involves mixing clay material and sawdust according to specific proportions, fusing with water, casted or molded and then allowing them to dry for approximately four weeks before firing is done to burn off carbonation material at 900^{o}C [20].

2.2 Mechanism of Ceramic Water Filtration

The main driver for the mechanism for filtration action is gravity. Water is pushed down with the force of gravity. The microporous material created through the combustion of sawdust provide interconnected pores which enhance to tortuosity of fluid flow. The water then interacts with the colloidal silver (silver nitrate) impregnated within the filter to kills any bacteria within the water.

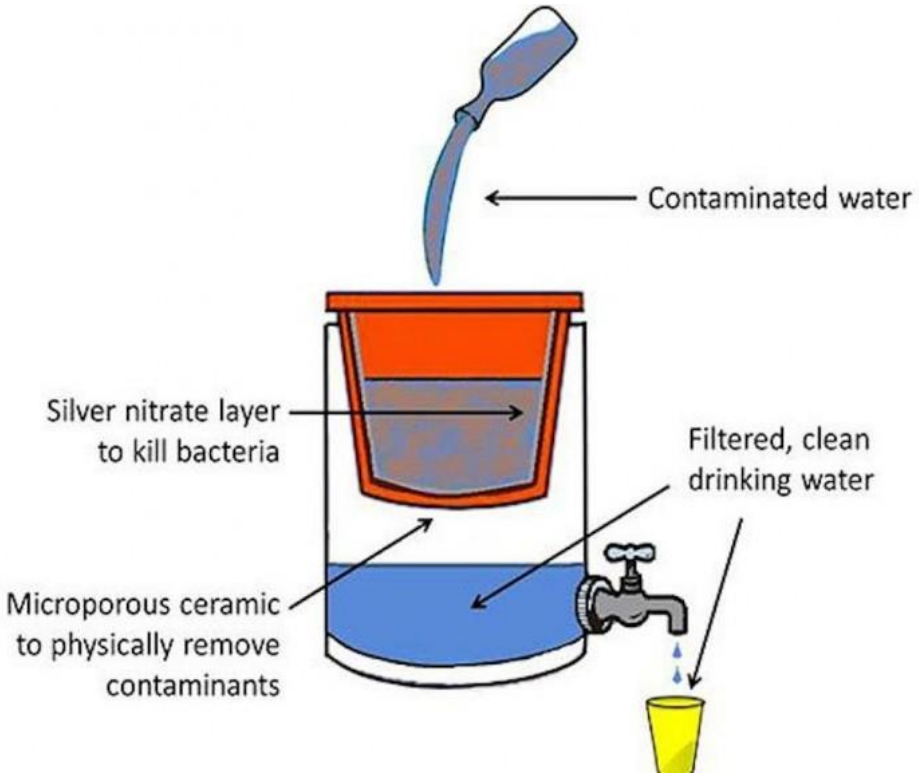

Figure 2.1: *Ceramic Water Filtration [21]*

2.3 Ceramics-Clay Materials

Being one of the most prevalent items in our society today, ceramics are essentially a variety of brittle, heat-resistant materials that a formed when a non-metallic mineral is molded, shaped, and fired. They are usually characterized by their physical properties. That includes their brittle nature, high melting points, relatively durable, high strength, hardness low thermal conductivity, and amongst others [22]. Being organized into two main groups of traditional and advanced forms, ceramics have evolved into a relatively large umbrella term for several materials including glass, porcelain, bricks, and pottery. Traditional ceramics are said to be clay-based and are classified as earthenware, stoneware, and porcelain. Advanced ceramics are usually classified as oxide-based, non-oxide based or combination [23].

Clay is one of the most versatile materials on earth, mainly due to its main physical property of high plasticity. It is a naturally forming material through the weathering of rocks. As a result of this, the usage of clay is highly adaptable, allowing it to be molded into various shapes and forms. Clay is composed of a mixture of fine-grain clay minerals and crystals such as carbonate, metal oxides, and quartz [24]. Clay is classified by a wide range of characteristics, including but not limited to its origin (primary or secondary), color, properties (plastic or short) and firing temperature (refractory or fusible) [25]. Based on these, we see clay being narrowly classified into three main sub-categories: earthenware, stoneware, and porcelain. Regarding the production of ceramic filters for water filtration, earthenware clay is most desirable due to its need for low firing temperatures, abundance in rural communities, and its high porosity [26].

Swanton [24] states that earthenware clay must be air-dried and then sieved to a specific micro-grain size using screens before use. This is done to ensure that the finest grains of the earthenware clay are in use, as particle size directly influences the plasticity, strength, and shrinkage of the clay mold to be produced, thus reducing inconsistencies and its susceptibility to failure. Each screen used for the filtering is known to have a maximum grain size through which it will permit easy passage, which is represented by the number of openings within one square inch. Potters For Peace (PFP) industry-standard ceramic filters use clay that has been sieved specifically between 60 mesh and then 35 mesh screens. This means that 60 mesh screens have 60 openings per square inch, ensuring that clay grains with diameters between 0.42 mm and 0.73 mm are the only size range of fine particles permitted through for use [25].

2.4 Composites Design

Composites combine two or more elements (or materials), each with different physical and chemical properties and compositions [27]. They are incredibly important materials used in

numerous applications such as aerospace, automobile, wood industry due to the combined strengths of each element incorporated within to create even better material for specific use products. Clay composites are usually created with a 3-part composition: the fiber, the binder, and water. The fibers serve as the main discernible reinforcing element, usually making up long strands in perpendicular or parallel orientations. The binder reacts to protect the reinforced phase from environmental conditions, while the water/resin aid the formation of a plastically deforming matrix. Clay materials contain iron in a specific quantity, which caused the reduction in the required maturing temperature. Hence, lead to an increased rate of production. Generally, composite design is often guided by the rule of mixtures equation as presented for the strength and modulus for both longitudinal and transfers loading [27].

2.4.1. Rule of Mixture

Rule of Mixture is used to determine the compositional factors and properties of a composite material. For the rule of mixture formulae to be presented, the focus was placed on transverse loading. The load will be applied almost directly perpendicular to the frames of the composite itself. As such, this transverse loading meant that the lower and upper bound Young's moduli are given by the formulas in equation 2.1a and 2.1b, respectively [27]:

$$E_c = E_m V_m + E_f V_f = E_m V_m + E_f (1 - V_m) \quad (2.1a)$$

$$E_c = \left(\left(\frac{f}{E_f} \right) + \left(\frac{1-f}{E_m} \right) \right)^{-1} \quad (2.1b)$$

$where\ f = \frac{V_f}{V_f + V_m}$, E_c is the modulus of the composite, E_f is the modulus of fiber, E_m is the modulus of the matrix, V_f is the volume fraction of fibers, and V_m is the matrix volume fraction. Moreover, the strain and strength of the composites in the lower (iso stress condition) and upper bound (iso

strain condition) are respectively given by equations (2.2a and 2.2b) [27]:

$$\sigma_c = \frac{P_c}{A} = \frac{(P_m)}{A} = \frac{(P_f)}{A} = \sigma_m = \sigma_f \quad (2.2a)$$

$$\varepsilon_c = f\varepsilon_f + (1-f)\varepsilon_m \quad (2.2b)$$

where P_c is the load of composite, P_m is the peak load of the matrix; P_f is the peak load of the fiber, σ_m is the strength of the matrix, σ_f is the strength of the fiber, ε_m is the strain of the matrix, and ε_f is the strain of the fiber.

It is to note that when the matrix is formed, we still have each element being easily recognizable and usually intertwined within different elements, with some of their most common benefits being the fact that they usually have relatively high durability, high impact strength, corrosion resistance, and in most cases, serve as insulators. With a wide range of uses, some of the most prevalent composites used today include fiberglass, plywood, reinforced concrete, and ceramic-matrix composites.

2.5 Ceramic-Matrix Composites

Ceramic-matrix composites refer to composites comprised of a ceramics-based matrix to provide binding when mixed with reinforcing material which could be particulates/fibers of ceramics/non-ceramic origins [28]. They are usually sighted to be porous and have a 'micro-cracked matrix,' introducing high anisotropy and, consequently, fracture toughness [29].

2.6 Combustible Material and Flow Properties

The production of ceramic filters relies heavily on the incorporation of combustible materials in the clay during production. Combustible materials are the particles that will combust and disintegrate during the firing of the clay composite to create a porous structure through which

water will flow during filtration. The existence of a wide range of combustible materials such as sawdust, rice husk, wheat flour, and cornflour indicates the existence of a range of particle sizes. This directly influences the pore sizes of the filter. For this to work, the combustible material is dry mixed with clay and any other material to form the composite. It is then wetted, molded, dried out before firing at a very high temperature, where this material combusts.

2.6.1. Saw Dust

Sawdust is the by-product of a range of woodworking operations, such as the cutting and machining wooden products. Its prevalence and abundance due to its mass production. Sawdust is composed of cellulose, lignin, and minor amounts of extraneous materials, with chemical compositions made up of carbon, hydrogen, oxygen, and minute amounts of nitrogen [30]. With an average diameter of 10 – 30 μm [31], and in some cases, 5 μm, sawdust can be seen to have a relatively fine particulate matter that can easily mix with clay and create the pores necessary for filtering.

2.6.2. Pore Size and Porosity

Pore size in ceramic filters is one of the most important structural factors in production. This is because the pore size determines what exactly will be let through into the filtered product. The conflict of interest here lies with what is being filtered and the flow rate. Microorganisms such as bacteria having an average size ranging from 0.3 to 100 μm and viruses with 0.02 and 0.2 μm [26]. The wide range between the varying sizes indicates that if these filters were to filter every microorganism out of water, the pores would be too small to have a sufficient and sustainable flowrate. As such, Potters for Peace (PFP) set the cap on pore size not to be larger than 3 μm [32]. Zereffa and Bakalo [33] show us an indication of how compositions affect porosity, consequently

affecting flowrate. Their filters included different compositions of clay, sawdust and grog, as shown (Table 2.1)

Table 2.1: Composition of Clay, Sawdust, Grog and Sintering Temperature [33]

Filter Code	Clay, wt.%	Saw Dust, wt.%	Grog, wt.%	Sintering Temperature, °C
C70-900	70	25	5	900
C70-950	70	25	5	950
C70-1000	70	25	5	1000
C75-900	75	20	5	900
C75-950	75	20	5	950
C75-1000	75	20	5	1000
C80-900	80	15	5	900
C80-950	80	15	5	950
C80-1000	80	15	5	1000

The filters, their codes, corresponding flowrate, and porosity are as given (Table 2.2):

Table 2.2: Summary of Flow Rate, Total Coliform, E.Coli, and Turbidity Removal Efficiency of the filters [33]

Filter Code	Flow Rate (Ml/H)	Total Coliform Efficiency (%)	E. coli removal (%)	Turbidity Removal Efficiency (%)	Porosity (%)
C70-900	400.00 ± 2.64	80.00 ± 1.00	83.78 ± 1.73	58.62 ± 1.00	65.43 ± 2.04
C70-950	340.00 ± 1.73	83.75 ± 2.64	89.18 ± 1.00	65.62 ± 2.64	52.65 ± 1.42
C70-1000	300.00 ± 5.29	87.50 ± 2.64	86.48 ± 1.00	67.25 ± 1.00	53.71 ± 1.86
C75-900	300.00 ±1.00	88.75 ± 1.73	89.18 ±2.00	70.68 ± 1.00	58.61 ± 0.91
C75-950	250.00 ± 1.73	91.25 ± 1.00	94.59 ± 1.00	89.65 ± 1.73	50.55 ± 1.84
C75-1000	250.00 ± 1.73	93.75 ± 1.00	93.24 ± 0.00	84.48 ± 1.00	50.62 ± 3.22
C80-900	250.00 ± 2.00	90.00 ± 1.00	91.89 ± 1.73	79.31 ± 1.73	60.74 ± 2.11
C80-950	200.00 ± 1.73	93.75 ± 1.73	95.94 ± 1.73	81.31 ± 1.00	49.43 ± 1.55
C80-1000	200.00 ± 2.64	96.25 ± 1.73	97.50 ± 1.73	87.93 ± 1.73	49.13 ± 0.98

The amount of sawdust (combustible material) decreased within the composite; therefore, porosity decreased alongside the flowrate. While porosity influenced what could be filtered out,

some experimentation suggests that even filters with larger pores than the size of microorganisms present within the water could be filtered. This was attributed to diffusion, inertia, turbulence, including other mechanical screening processes [34].

2.6.3. Factors Affecting Flowrate

PFP states that flowrate measurements are mainly for quality control. One identified factor that affects flowrate is the frequency of which it is cleaned after consistent use. Swanton [26] identified that filters had an increase in efficacy in the successive days after it was cleaned of the sludge and leftover particles, following a month of consistent use. This was backed by the increase of two filters' flow rates from 0.4 L/hr and 0.28 L/hr to 2.1 L/hr and 2.0 L/hr, respectively, after the appropriate method of scrubbing was performed on these two filters [35]. Particle size, viscosity of the water due to particles and substances present within it, and the coarseness of particles are some other factors that influence the flow rate within a ceramic filter.

2.7 Effects of Temperature

Clay is a very stimuli-sensitive material in that many things can affect its immediate properties. One of such is temperature. In the production of ceramic filters, where clay is used, firing is required to further dry and harden the clay, as well as to burnout the reinforced material to enhance the porosity of the filter. When being fired in a kiln, it is essential to monitor the temperature levels and raise this temperature at a steady rate to prevent excess water from turning into steam. This could be detrimental for the clay as it causes explosiveness within the clay, causing cracks and failures. There is a need for the filter to be of a certain strength level and this maturation of the clay only occurs at a specific temperature, depending on the specific type of clay.

Temperatures above this maturation temperature can cause the clay itself to melt, causing undesired deformation [36].

2.8 Manufacturing Processes for Mechanical Optimization

In the context of this project, we can define optimization as the attempt to find the geometric configuration that would reduce the pressure drop of water as it goes through the filter while ensuring that there is maximum surface area contact between the water and the filter itself. As such, we need to explore certain manufacturing processes that would support this. A combination of porosity and mechanical strength would support the choice of composite structure to develop the filter.

2.8.1. Compression Molding

Compression molding (Fig. 2.2) is the process of putting a large, usually rounded slab of the mixed composite into a cavity with the aid of a press to take the shape of that specific cavity, wherein this case, would be the pot shape chosen for the ceramic filter. Most production facilities use manual hand-pressed techniques to cut down cost. This leads to some inconsistencies within the mold [25].

***Figure 2.2**: Compression molding is the process [37]*

2.8.2. Automation

The introduction of automation within press systems would reduce the inconsistencies associated with dimensioning, especially with regards to the filter thickness. Filter thickness could be a determining factor between whether or not the filter could structurally fail during the sintering process, when being handled or during transportation. The PFP Dutch Press is an example of a system that makes use of hydraulics, designed with a 20-ton capacity jack [25]. Though this makes it easier to lift, the introduction of automation allows for a consistent spread of the clay composite in the molding process. Clay particles are known to laterally arrange themselves perpendicularly to the pressure being applied to them [25], with some mixture inconsistencies sometimes causing molding to be a little on the tougher side. A system that incorporates automation within it would enable it to know the amount of force being applied to counteract the resistance against it, allowing for easier molding.

CHAPTER THREE

3.0 Design and Methodology

3.1 Design Requirements

The design process required some systematic run through the usage of water, how it is used, down to how much an average family within a rural community uses water daily. A study in the Eastern Region of Ghana indicates that out of 74 different towns, 5044 households, each household consumed an average of 203.75 m^3 of water monthly [38]. These figures translate to a daily average of 6.79 m^3 of water. Considering the 2010 Population and Housing Census reports that an average household in an Eastern Regional rural community comprises 4.1 people [39], this is an indication that each member of the household uses 1.6975 m^3 of water per day. With a total of 47.2% of their supply comprising of water from rivers, dugouts, unprotected wells, rainwater, and borehole [39], there is a relatively prominent level of uncertainty with regards to how clean the water is for consumption. Hence, the need for a specific process to clean this water to an extent makes it safe for drinking and domestic consumption.

Based on analysis of basic average human activity, a flowchart indicating the daily processes of water usages was generated, as shown in Fig. 3.1

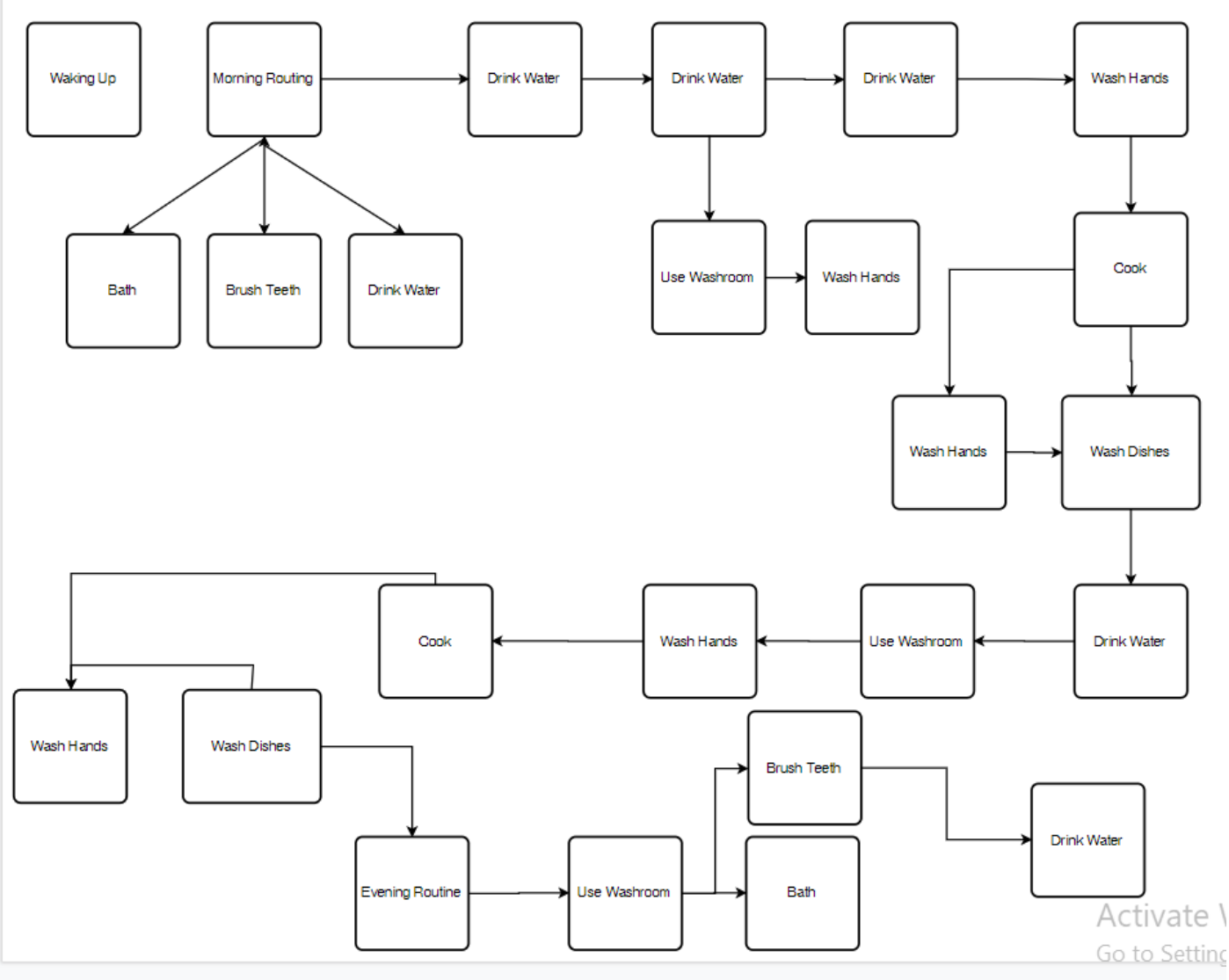

***Figure 3.1**: Estimate the Daily Process of Water Usage*

From the above flowchart, we see a total of 16-23 points where each person would require the usage of water. This translates to 0.0786 m^3 (78.6 L) - 0.118 m^3 (118 L) of water needed to be filtered at each point in time. From this value, there is a need to determine if this will be infrastructurally possible.

With the first set of data presented in Table 3.1, we see that the range for the flowrate of the Potters for Peace ceramic filters is averaged to be between 0.62-2.522 L/hour with an average of 1.448 L/hr. The infrastructural flowrate of the PFP as 1.448 L/hr means that filtering water for

all 16 points of the need of water will not be possible to meet the daily water consumption for a household, provided only one filter is in use.

Table 3.1: Flow Rate of Potters For Peace (PFP) Filters [26]

Location	Source	Number Of Filters	Lab/Field	Range (L/hr)	Average (L/hr)
Ghana	Matellet, 2005	3	Lab	0.48 – 19.91	1.06
Ghana	Van Halem, 2006	7	Lab	1.05 – 4.29	2.41
Nicaragua	Lantagne, 2001	24	Field	0.13 – 3.5	0.98
Nicaragua	Van Halem, 2006	7	Lab	0.51 – 1.45	0.85
Cambodia	Van Halem, 2006	8	Lab	0.51 – 1.14	0.73
Cambodia	Brown, 2007	1	Lab	1.5 - 2	1.75
Burkina Faso	Piaskowy, 2008	2	Lab	0.16 – 3.37	0.61
Guatemala	ICAITI, 1984	1	Lab	N/A	3.5

There is now a need to identify the critical paths of water, which would specifically be drinking water. With the average recommendation of the amount of water drank per day standing at eight (8) 8-ounce glasses, or an equivalent of 2 litres, there is the need for each person to drink water at least eight times a day (8.2 litres/per person).

With an average flow rate of 1.448 L/hour, assuming a 4-hour cycle, 5.79 litres of water can be filtered. Assuming each person drinks 0.25 litres of water every 1.5 hours, they require 0.75 litres every 4 hours. This means that, for each 4-hour water filtration cycle, with 5.79 litres of water being filtered, only 3.075 will be consumed, leaving 2.717 litres left for any other purposes. This gives a water supply safety factor of 1.1318.

From this, the whole storage container + the ceramic filter as a unit has a total capacity of 6-8 litres. This can be seen as an adequate volume for a household, provided they were to top up the filter with water 2-3 times a day.

3.1.1. Designing for Volume Requirement

Identifying that the unit must hold a mean of 8 L of water, a breakdown is required on the feasibility of this. For a contextually acceptable storage container, the setup of a *Veronica Bucket* was used, a transparent bucket that has been fitted with a spigot, or tap opening, at the bottom of it for easy access to flowing filtered water.

To proceed with the design process, we needed to determine the shape of the filter from the proposed sketches. Non-dimensional shape sketches were produced, as seen below.

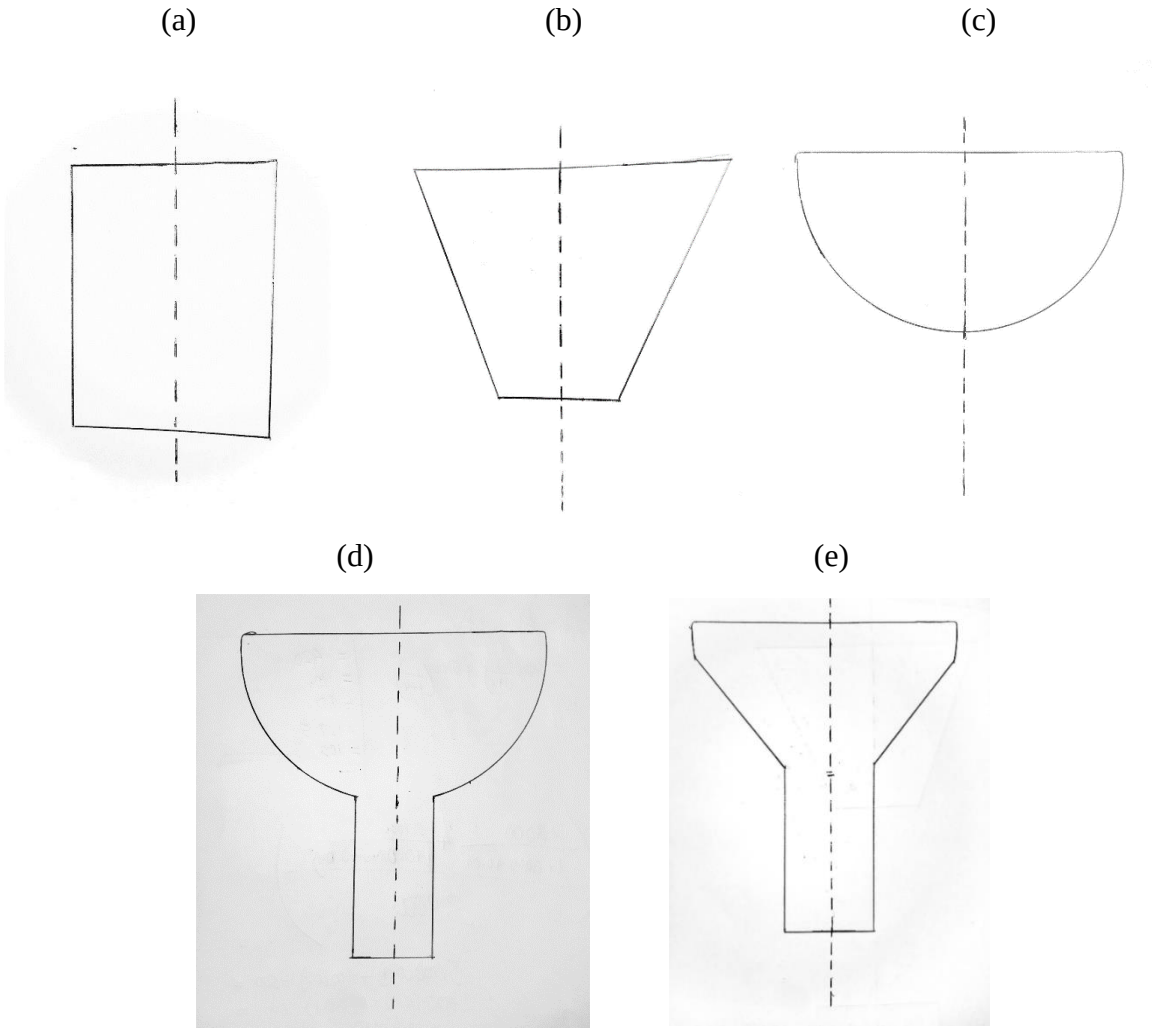

Figure 3.2*: Evaluation of Proposed Filter Shapes: (a) Shape 1, (b) Shape 2, (c) Shape 3, (d) Shape 4, and (e) Shape 5.*

A Pugh Chart (Table 3.2) was used as an evaluative matrix to determine the best shape sketch for the final designs. A scoring system of 1-5 was used, with the highest total representing the best shape, while the lowest of the least shape would be discarded. The 'critical point' column is inverted with a higher value indicating less critical points meaning that less susceptibility to failure when loading is applied. For force distribution, some models were done in CAD software (SolidWorks 2020 package) using a controlled diameter of 30cm, which served as the controlling dimension for the other dimensions. Static analysis was done with the force of gravity and a downward distributed mass (Fig. 3.3) of 6kg applied on shape models. All the shape sketches were fixed at the bottom, except for Fig. 3.2.c, fixed on the round edges. A solid mesh with an average of 16000 nodes per mesh was used before the simulation was run. The material in Solidworks 2020 was ceramic porcelain, with

(a)

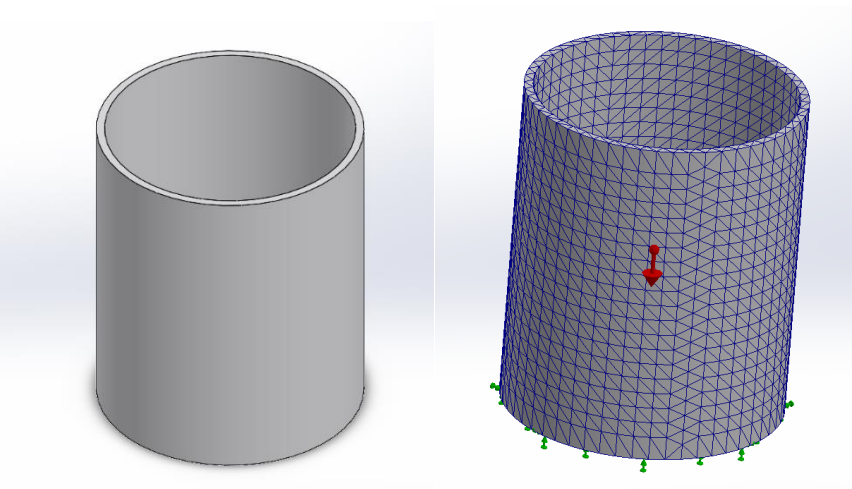

(b)

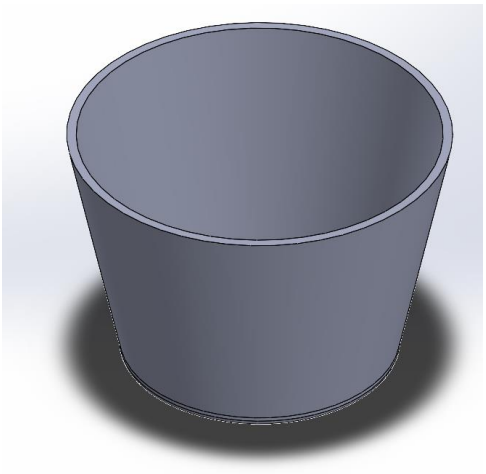

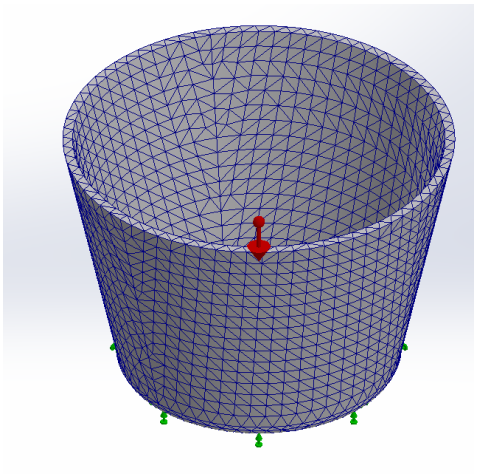

(c)

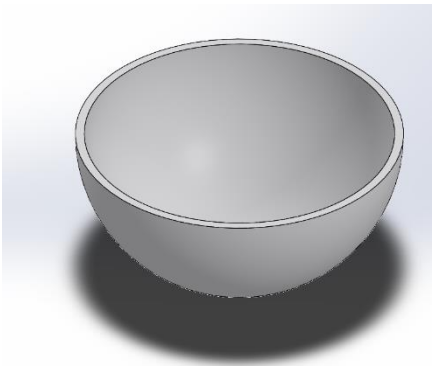

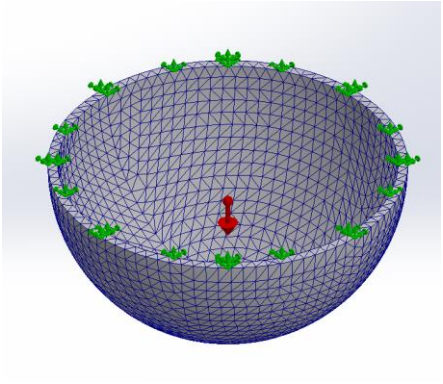

(d)

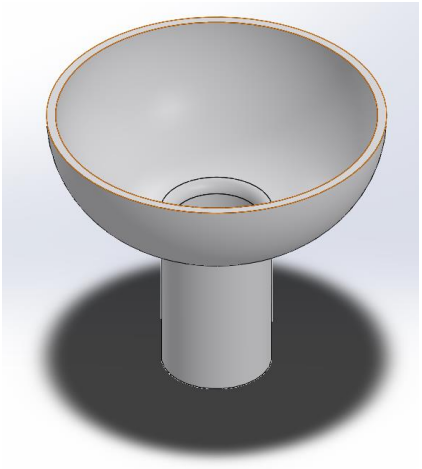

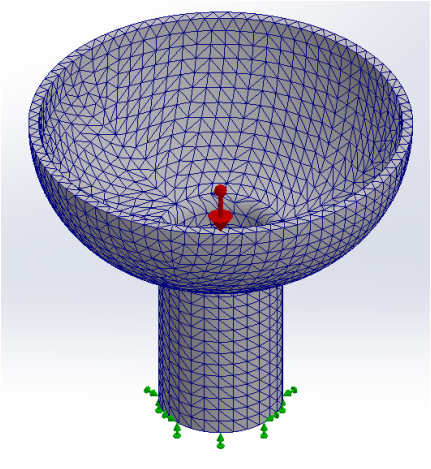

(e)

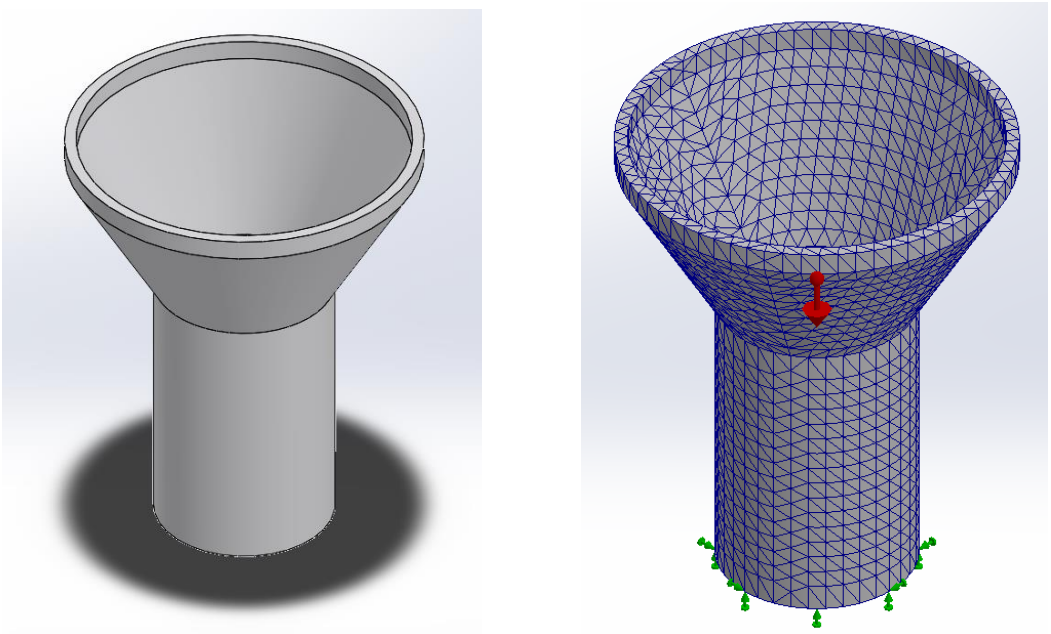

Figure 3.3*: 3D SolidWorks Models of Proposed Shape Sketches for Design Selection with Mesh Application: (a) Shape 1, (b) Shape 2, (c) Shape 3, (d) Shape 4, and (e) Shape 5*

Table 3.2: Pugh Chart for choosing appropriate shape sketch**.**

Parameter	Aesthetics	Surface Area Available for Filtration Action	Stress Distribution	Critical Points	Storage Ease	Total
Shape 1	1	2	1	4	4	12
Shape 2	4	4	3	4	5	20
Shape 3	5	5	5	5	5	25
Shape 4	4	2	5	2	1	14
Shape 5	2	1	3	1	1	8

From this Pugh Chart, we can notice that shape sketches 3b and 3c (trapezoidal/truncated cone and semi-oval/hemi-ellipsoid) were the best ones to use in the design process.

Coming back to the need for the filter to have a maximum volume of 7 litres, we can continue the design process by calculating for the corresponding dimensions.

Starting with shape 3b, a truncated cone shape (frustum) structure was obtained. The volume is given by the formula [40]:

$$V = \frac{\pi h}{3}(r^2 + R^2 + rR) \quad (3.1)$$

where r is the radius of the base, R is the radius of top, and h is the height of the filter.

Acknowledging that a relatively large surface area for filtration is expected, the design considers factors such as a large taper angle or a large circular base area. These two considerations would greatly affect the height of the filter, and they are both driving factors for the final shape.

3.2 Effect of the Taper Angle on Stress Concentrations

SolidWorks simulation on the effect of tapered angles on increasing stress risers was carried. As there is a presence of highly localized stresses when there is an immediate change in a structural member, we need to analyze the effects of this discontinuity on the model itself [41]. As such, the diameters of the individual filters were kept constant, while the tapered angles were varied at 10^o, 20^o, 30^o, and 42^o. Also, two filter heights were considered (20 cm and 30 cm). This alters the critical locations of the filter. A Pugh Chart for choosing the appropriate tapered angle is presented (Table 3.2). The filter was then modelled with the fixtures placed right under the handle edge of the filter. The simulated samples were probed on SolidWorks and graphically compared the effect of tapered angle on the stress concentrations on the filter. Similarly, the effect of height was also compared.

For the simulations, the material specified had to emulate clay material properties. With SolidWorks 2020 not having an appropriate clay material for selection, Amazian's [42] research on *Unfired Clay Bricks with Enhanced Properties* cites Stephen Guggenhiem's research on montmorillonite as the main material within clay minerals, and as such used data presented in their findings as the data to generate earthenware clay's main material properties.

Table 3.2: Table of Material Properties for Earthenware Clay, Based on Data from Red Montmorillonite [42]

Material Property	Value
Elastic Modulus	50 GPA = 50 000 N/mm^2
Poisson's Ratio	0.26 N/a
Shear Modulus	16.4 GPA = 16 400 N/mm^2
Mass Density	2.3 g/cm^3 = 2 300 kg/m^3
Tensile Strength	30 N/mm^3
Specific Heat	1 100 J/(Kg.K)
Thermal Conductivity	1 W/(mK)
Thermal Expansion Coefficient	20/K

Table 3.3: Pugh Chart for choosing appropriate Tapered Angle**.**

Parameter	Aesthetics	Surface Area Available for Filtration Action	Stress Distribution	Accurate Dimensioning	Storage Ease	Total
20 cm/10º	4	4	4	5	5	22
30 cm/20º	4	5	5	3	4	21

A trapezoidal design (Fig. 3.2.b) filter of height 20 cm, and a taper angle of 20º was selected for further mechanical investigations.

3.3 Design requirements

Below are presented as follows:

- The designed ceramic composites must fulfill all set criteria for mechanical properties with a combination of pore distribution with the matrix.
- The product must be relatively mobile and can render a 'drinking-water service' from existing water reservoirs, in accordance with WHO standards of (5-7 litres per hour) and an average industry-standard flowrate of 1.448 litres per hour.
- It must be relatively lightweight, cost-effective ($7 - $16), and low maintenance cost ($ 1-$16).

3.4 List of Materials

Clay and sawdust materials were sourced locally for the fabrication of the ceramic filters. Clay material was the primary matrix ingredient sourced from Afienya, in Tema, Ghana. The clay in its dry state is seen below (Fig. 3.4a). The sawdust used in this work was sourced from a town in the Ga Municipal District, Afuaman, within the Greater Accra Region from a sawmill. The sawdust (Fig. 3.4b) was produced as a derivative of wood pieces from the *Wawa* tree. This tree is known to be a leading export timber within West Africa and is said to be amongst one of the lightest hardwoods available.

(a) (b)

Figure 3.4*: Raw Materials for Clay Composite: (a) As-received Clay and (b) Collected Sawdust.*

3.5 Prototype Design Processes

Based on the shape sketches presented earlier and the corresponding Pugh Chart used for selection, the system was modelled after the frustum with a diameter of 40.6 cm (radius = 20.3 cm) and a taper angle of 20^{o}. Three-dimensional (3D) models were produced (**Fig. 3.5**). The volume of the filter was determined according to equation (3.1) above. The filter was designed with a height of 18 cm, a diameter of 30 cm, and a tapered angle of 20°. Since this was done manually, anomalies in dimensions could arise. In addition to catering for any expansion during forming and shrinkage during firing within the clay, a range of dimensions was then given:

- **Height:** 18 - 21 cm
- **Diameter:** 32-37 cm
- **Taper Angle:** 20 – 25 degrees

(a)

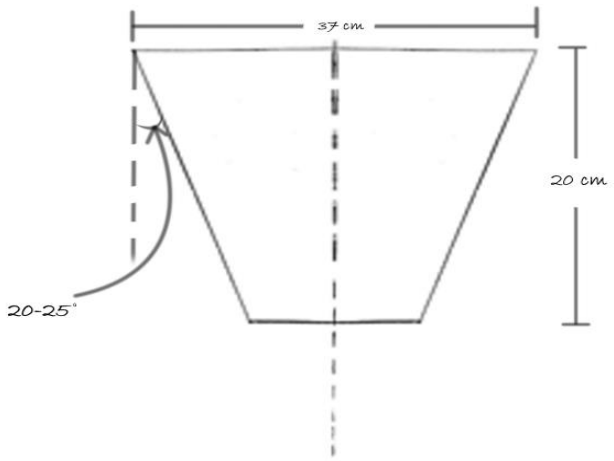

(b)

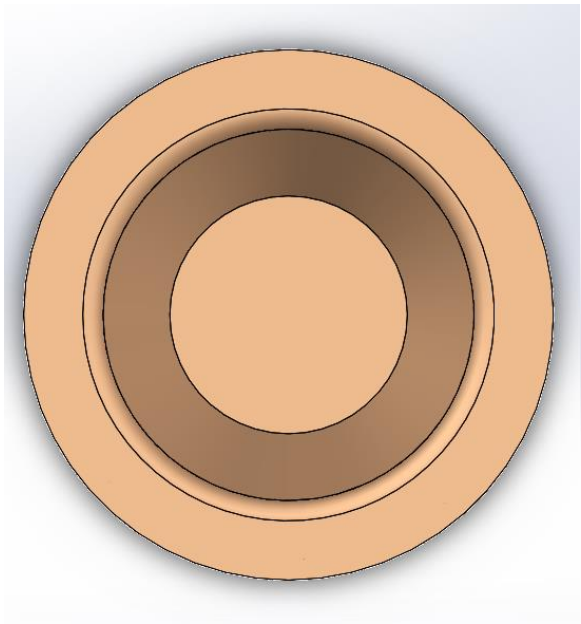

(c)

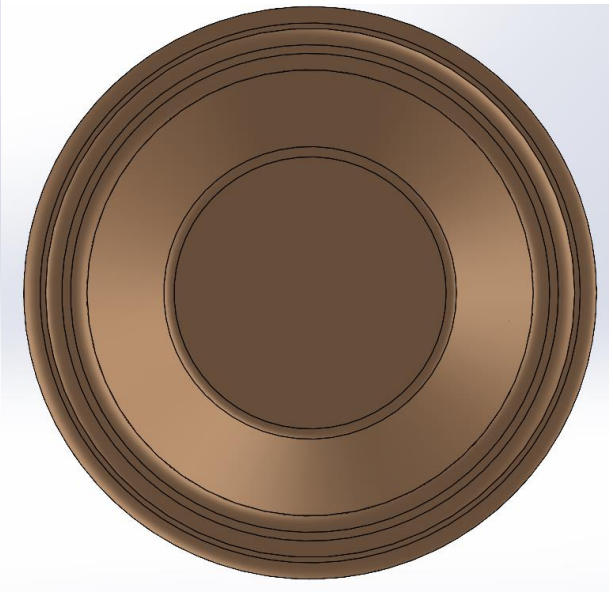

(d)

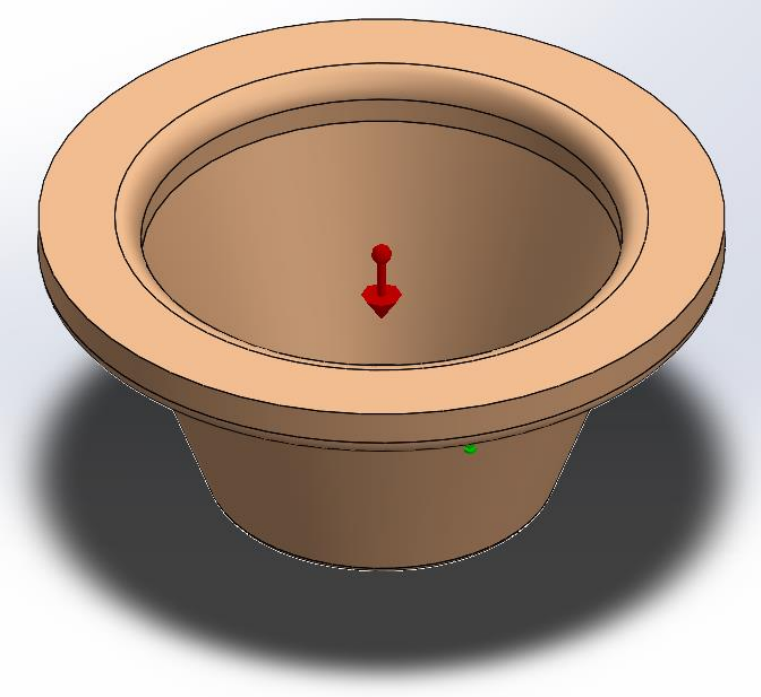

Figure 3.5*: Selected CAD Model for the Prototype: (a) Front View, (b) Top View, (c) Bottom View, and (d) Isometric View.*

3.6 Mechanical Optimization

To ensure that the design requirements were being met, some conditions were necessary to mechanically optimize the ceramic-based composites filtration (Table 3.3). To optimize the composite materials, the fiber volume fractions were varied as seen in Table 3.4 until a threshold in the percentage sawdust within the composite was discovered with difficulty to obtain a uniform mixture. The porosity was manipulated in this regard following the combustion process. Based on our chosen dimensions and based on the materials selected, we can find out about the filter. To run these tests, slabs were created for impact and drop tests.

Table 3.4: Design requirements for the Ceramic Filter

	Low	High
% increase in dimensions when fired	▼	
Apparent Porosity		▲
Toughness		▲
Bending Strength		▲

While a relatively high porosity is desired, it is essential to note that an inverse relationship exists between the porosity and the strength of the material. As such, a balance needs to be found where the porosity is chosen allows for a sufficient flowrate, while also ensuring that the composite itself is strong enough to withstand loading from everyday usage.

3.7 Mixture Compositions

The as-received clay was crushed and sieved into fine particles for use. Wood shards were removed from the sawdust collected by hand. Clay composites were formed by varying the volume fraction of the sawdust which acts as the reinforced phase. Different compositions were made using the rule of mixture. These compositions were given in Table 3.4. Slabs were then molded (11cm x 5cm x 3cm) (Figure 3.6).

Table 3.5: Composites Design and Respective Ratios

Slab No.	Clay (%)	Sawdust (%)
Control Sample	100	0
Composite 1	40	60
Composite 2	50	50
Composite 3	60	40
Composite 4	70	30
Composite 5	80	20

Figure 3.6: Selected Photograph of Freshly Applied Composite Slabs Before Molding and Forming Took Place

Figure 3.7: *Selected Photograph of Dried Composite Before Firing*

3.7.1. Dimensional Differences (Shrinkage Testing)

In determining the dimensional differences between before and after the filter was fired, the length of the slabs was taken before and after firing was done to determine any structural changes that might occur. The percentage change in length (%PL) is given by the following:

$$(\%P_L) = \frac{L_a - L_b}{L_b} \quad (3.2)$$

where L_a is the length after firing and L_b is the length before firing.

3.7.2. Apparent Porosity

In determining the flow rate of the filter, it was necessary to determine the porosity and water absorption of the filter. The slabs obtained were used. Their masses before, during, and after being soaked water for 16 hours were recorded. This information was used to determine the pores' water retention levels. As no mechanical balance system was available to measure the suspended mass of the slab, improvisation led to the use of equivalency, where a pulley was placed with two strings on either side of it; one end holding up the suspended slab immersed within the water, and the other end holding up a combination of items that were equivalent to the mass of the suspended slab. Upon achieving equilibrium, the mass of that combination of items was measured like regular mass to determine how much the suspended mass itself was.

To calculate this analytically, based on the material chosen, the formula provided is as per the Standard Test Method for Water Absorption, Bulk Density, Apparent Porosity, and Apparent Specific Gravity of Fired Whiteware Products ASTM-C 373-88, 2006 [43].

Apparent Porosity was given by:

$$\eta(\%) = \frac{M_{sa} - M_d}{M_{sa} - M_s} * 100 \quad (3.3)$$

where M_{sa} is the saturated mass, M_d is the dry mass, and M_s is the suspended mass in water.

Water absorption was given by:

$$Water\ Absorption = \frac{M_{sa} - M_d}{M_d} * 100 \quad (3.4)$$

3.8.3. Toughness

Understanding the extent and mechanics of failure would enable us to determine the most appropriate composite ratio due to the extent of damage caused under specific tests.

3.8.3.1 Impact Loading

Impact testing of the clay slab would be able to determine the strength and toughness of the clay slab, as it essentially shows the necessary forces required to instantaneously cause failure through fracture to the slab. This test occurs by fixing the slab in place and dropping objects of a controlled mass perpendicular to the slab at a specific height. When the object hits the slab, it can be seen to transfer energy to the slab. This now-absorption of energy from the slab causes yielding to occur, and eventually, when no more energy can be absorbed, fracture. This consequently causes plastic deformation at the infinitesimal point of contact.

Being a qualitative point of analysis, the crack propagation and extent of fracture would be used to determine which composition is the best to be used.

3.8.3.2 Drop Test

Much like the impact test, there is a need to analyze the extent of damage to the clay pot in use and as such, this drop test would help determine which composite ratio is most appropriate based on its shatter or damage when the brick is dropped from a specific height, for each composition. With the slabs in a horizontal orientation, this allows for the slabs to land directly on their faces and to determine the extent of damage the drop has on it. The height set for the drop was 1.3 metres from the ground. The slab would be raised to that height and released for free fall and the force of gravity being the downward force. This would be repeated for all slab compositions in Table 3.5.

3.8.5 Preliminary Hardness Test

This test is designed to be a qualitatively binary test for hardness as it requires a fingernail to be scratched upon the finalized slab. A significant difference made on the slab from that scratch means that the slab is not hard enough.

CHAPTER FOUR

4.0 Results and Analysis Discussion

4.1 Mechanical Computational Simulation Analysis

Using CAD software (SolidWorks 2020 package), some models were generated based on the shape sketches provided in Fig.3.2, the dimensional sketches in Fig. 3.3 and consequently, the finalized design in Fig. 3.5, with analytical emphasis placed on the loading conditions and stress concentrations.

4.1.1. Effect of Shape on Stress Distribution

(a)

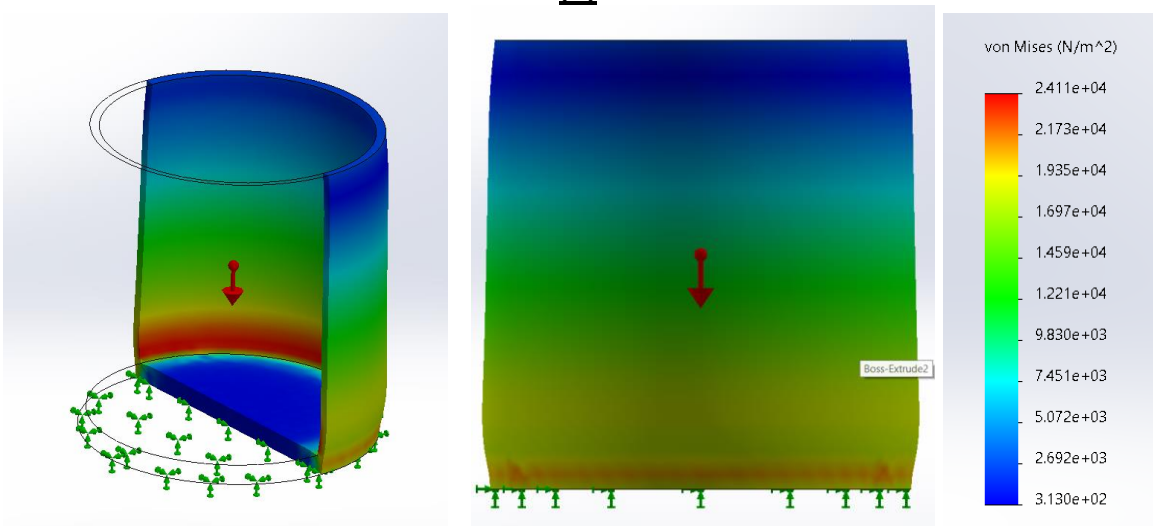

(b)

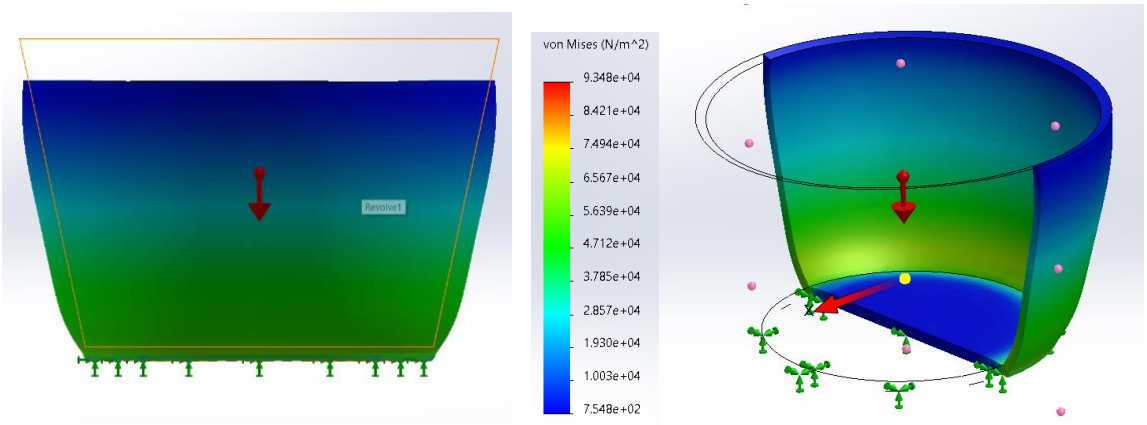

(c)

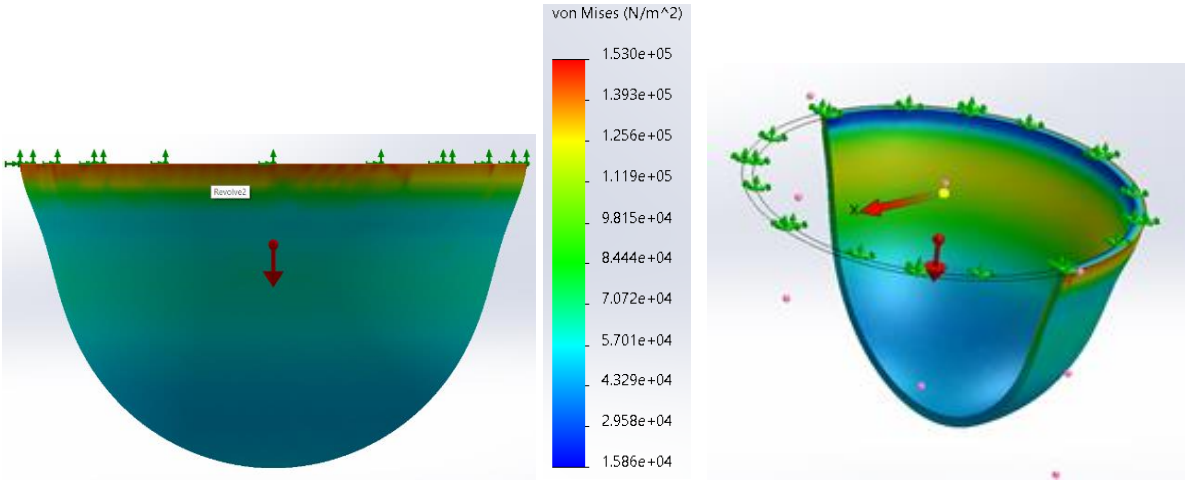
von Mises (N/m^2)
1.530e+05
1.393e+05
1.256e+05
1.119e+05
9.815e+04
8.444e+04
7.072e+04
5.701e+04
4.329e+04
2.958e+04
1.586e+04

(d)

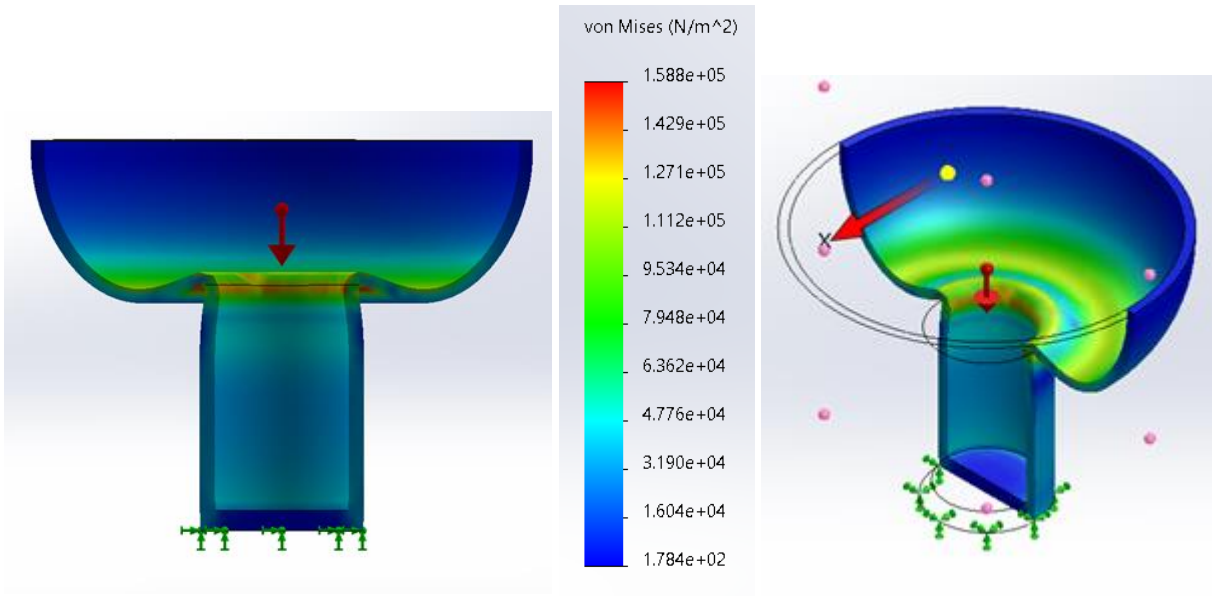
von Mises (N/m^2)
1.588e+05
1.429e+05
1.271e+05
1.112e+05
9.534e+04
7.948e+04
6.362e+04
4.776e+04
3.190e+04
1.604e+04
1.784e+02

(e)

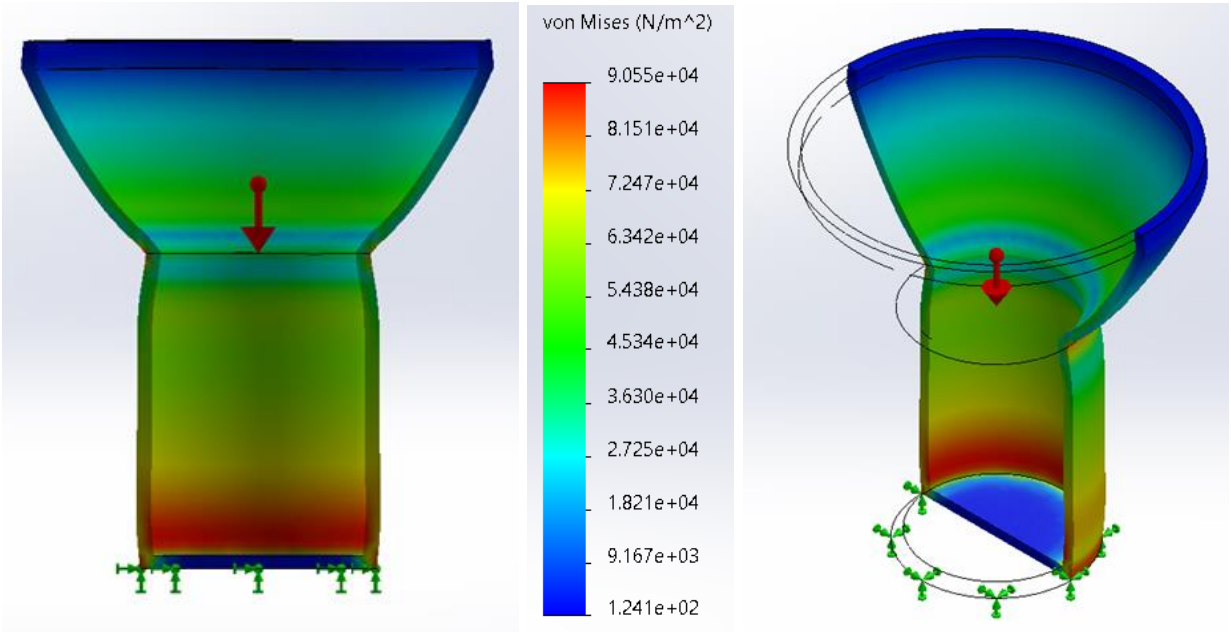

Figure 4.1.1: *3D Solidworks Visualization of Stress Distributions, Corresponding Von Mises Stresses and the Section View: of each shape sketch model: (a) Shape 1, (b) Shape 2, (c) Shape 3, (d) Shape 4, and (e) Shape 5*

The introduction of the shape sketch analysis was done to determine the stress distributions over each model of the shape sketch to see which shape works best under a distributed load, or in this case, a full capacity of water. Shape 3 and shape 4 undergo the highest level of Von-Mises stresses, with the former having this peak of 1.53 N/m^2 occurring on the edge of it. There is evidence of buckling within each of the models run, and this can be attributed to the lack of reinforcement or a relatively small thickness used in the modelling dimensions.

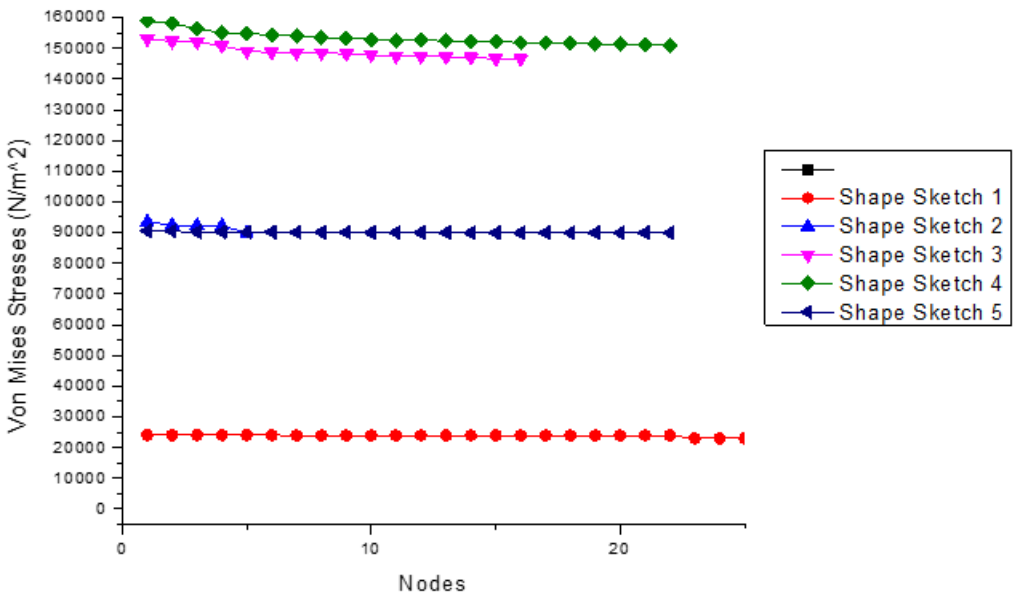

***Figure. 4.1.2**: Von Mises Stresses of Shape Sketches Plotted with respect to Their Nodes*

Graph 4.1 shows the peak of the Von-Mises stresses acting on each shape sketch. This graph shows that shape sketch 4 had the highest Von Mises stresses equivalent to 0.16 MPa. These shape sketches were dimensionally scaled down by a factor of 4.5, hence rendering them dimensionally inaccurate as compared to the chosen design in Fig. 3.5. As such, scaling the compressive strength of 30 MPa down by the same factor still means that the shape sketches would not undergo any failure through yielding.

4.1.2. Effect of Tapered Angle on Stress Distributions

Height: 20 cm

(a) 10 Degrees

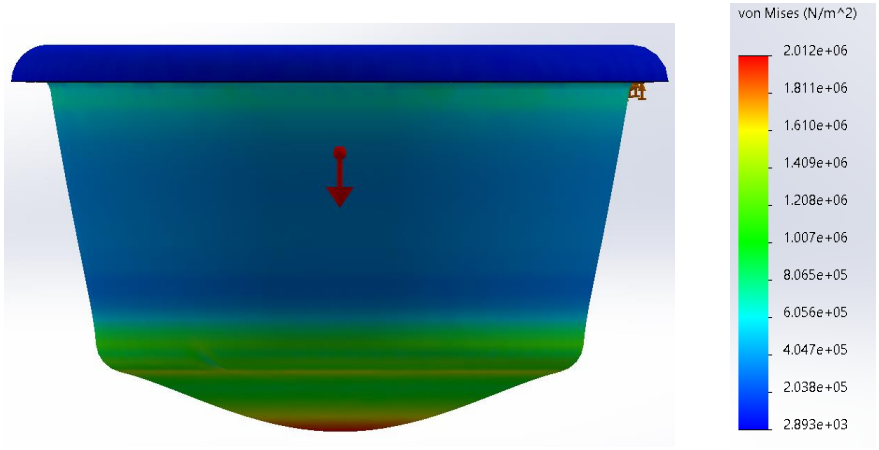

(b) 20 Degrees

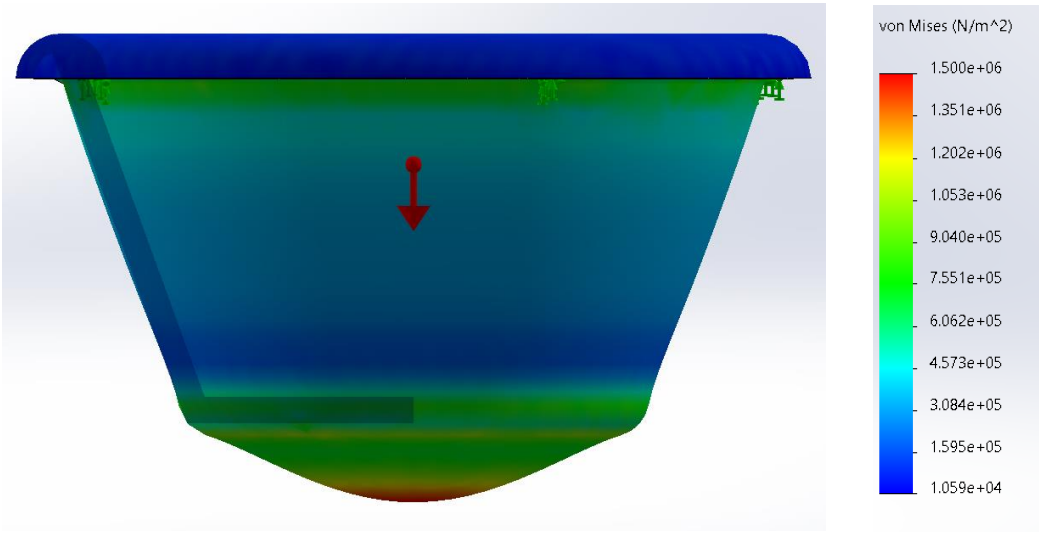

(c) 30 degrees

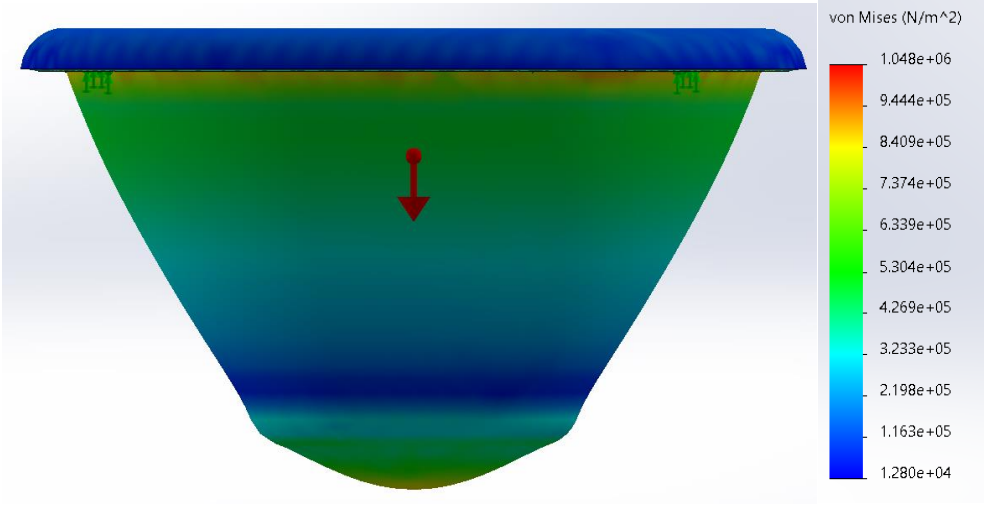

(d) 42 Degrees

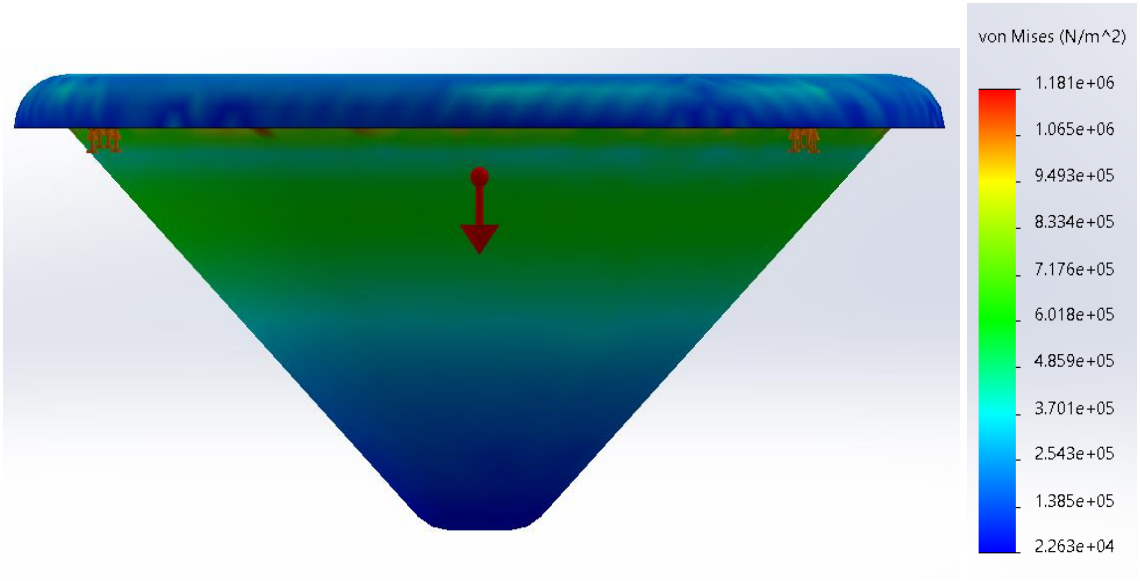

Figure 4.2.1: *3D Solidworks Visualization of Stress Distributions, Corresponding Von Mises Stresses and the Section View at a filter height of 20cm: (a) Shape 1, (b) Shape 2, (c) Shape 3, and (d) Shape 4*

The above shows the different stress distributions at different taper angles for a fixed height of 20cm. These simulation results show that increased the surface area on which gravity and downward-facing forces can act on the filter, as an inverse relationship with the peak of the Von Mises stresses acting through the distributed loading. The taper angle 20^{o} in Fig. 4.2-I (a) peaks with stresses of approximately 2.012 MPa falling to 1.048 MPa in Fig. 4.2-I (c).

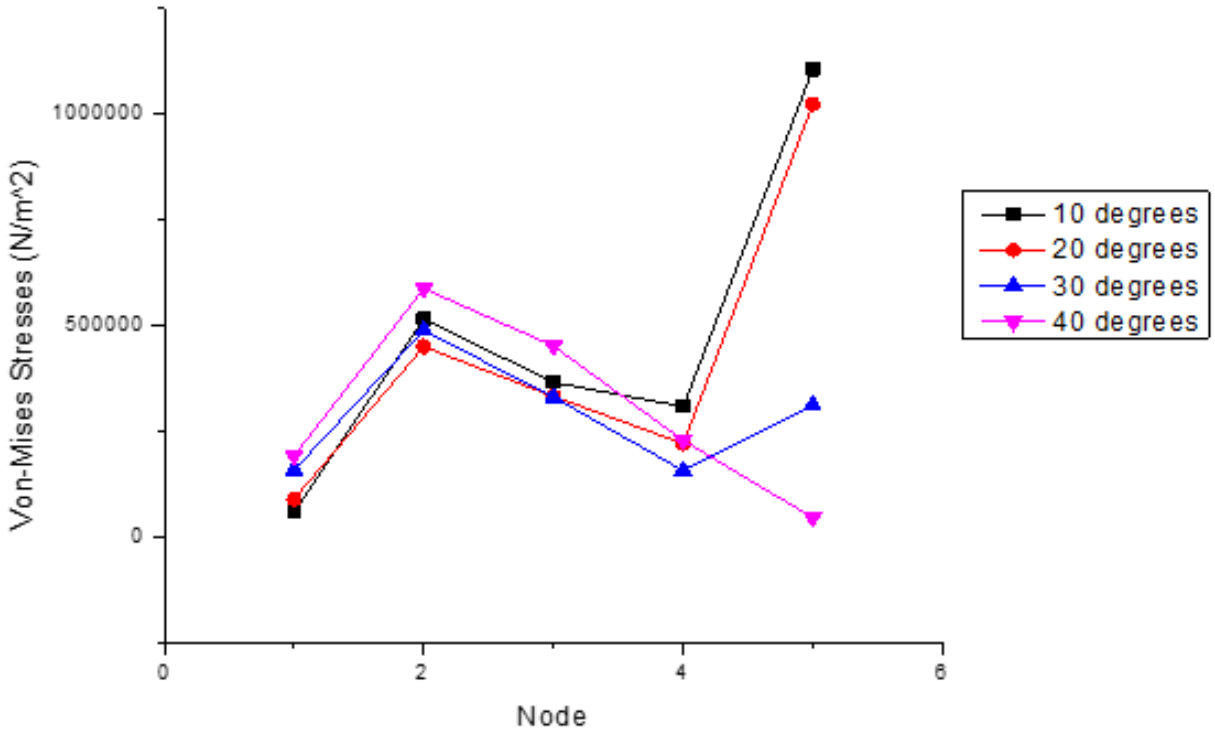

Fig. 4.2.2: *Graph Showing Probe Von-Mises Stresses in Descending Height throughout the filter with corresponding taper angles with a filter height of 20cm*

Fig. 4.2.2 shows the von-mises stress of filters of tapered angles 10^{o}, 20^{o}, 30^{o} and 42^{o}. These results were probed off five equally spaced points along with the height of each filter. At a filter height of 20cm, Fig. 4.2.2 shows that taper angles 10^{o} and 20^{o} are able to withstand higher Von-Mises stresses towards their base of the filters. The filter with a 42^{o} taper angle has an inverse result, as opposed to the other, and this can be attributed to the significantly smaller surface area of its base.

As such, the filters with 10^{o} and 20^{o} taper angles can be selected as ideal, with regards to the stress distributions.

Height: 30 cm

10 Degrees

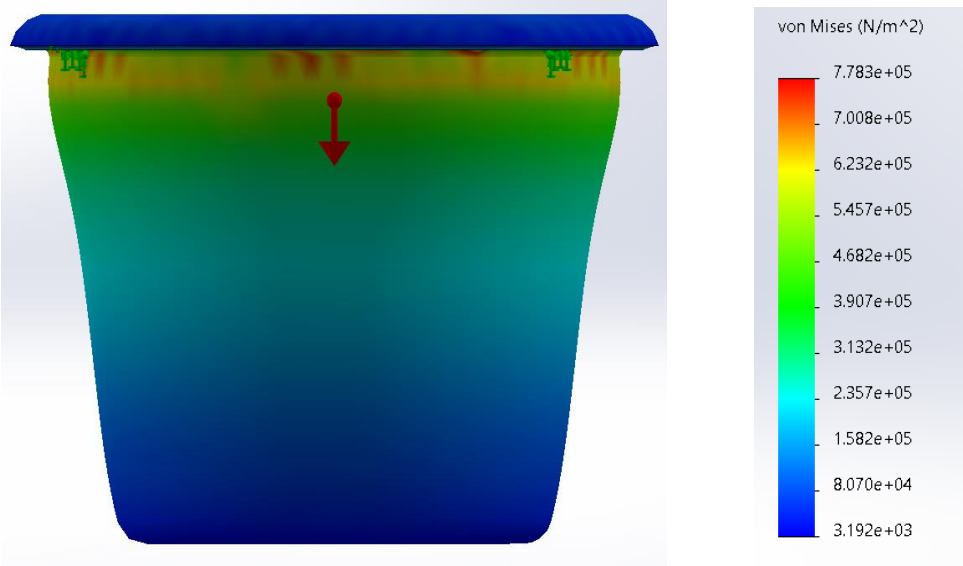

20 Degrees

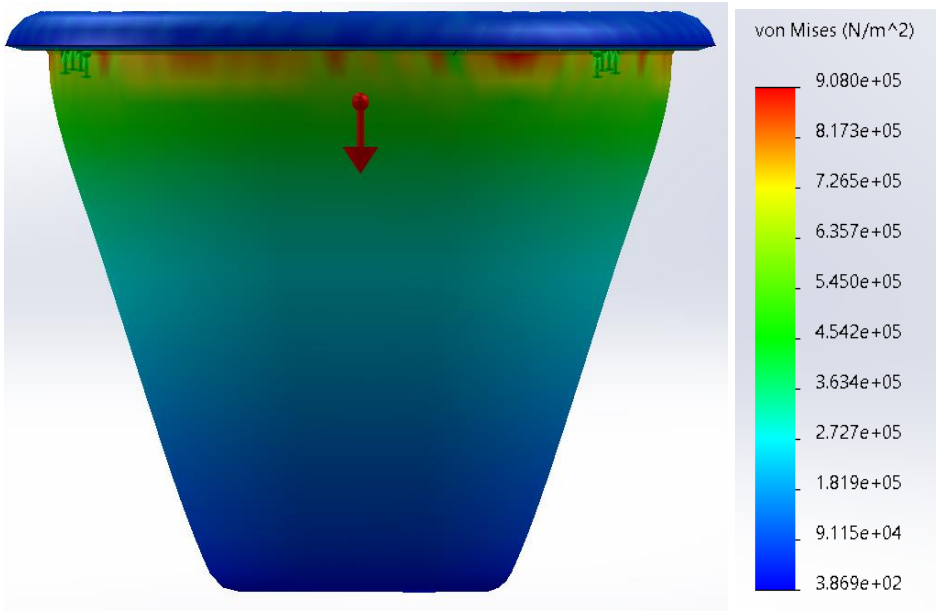

30 Degrees

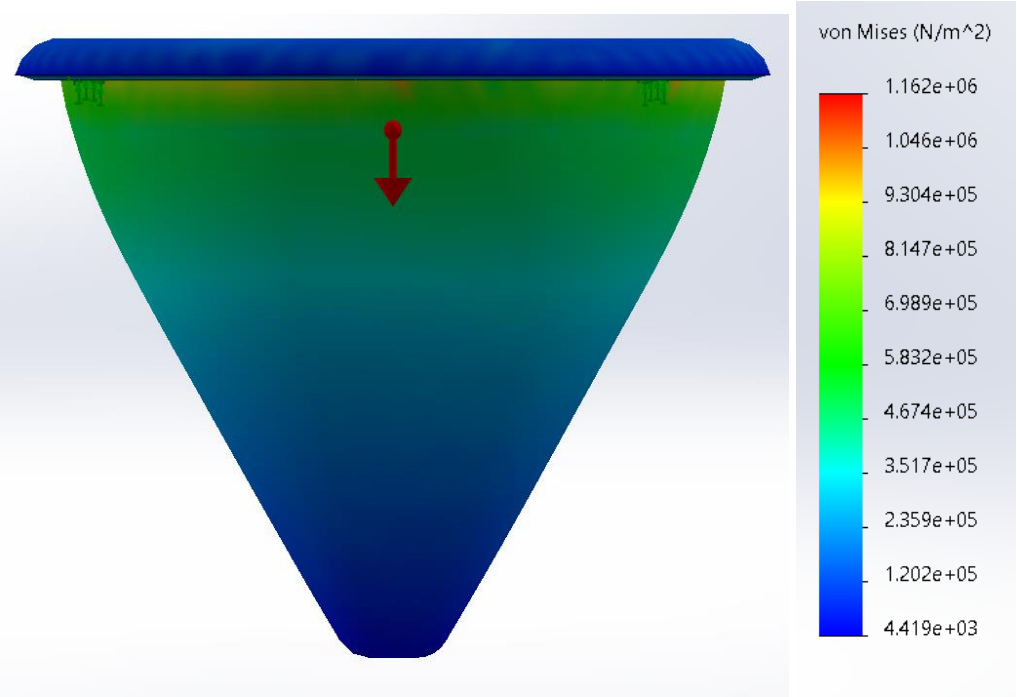

42 Degrees

(NULL) – NOT GEOMETRICALLY POSSIBLE

Figure 4.3.1: *3D Solidworks Visualization of Stress Distributions, Corresponding Von Mises Stresses and the Section View at a filter height of 30cm: (a) Shape 1, (b) Shape 2, and (c) Shape 3*

Simulation results in Fig. 4.3.1 go contrary to simulation results in Fig. 4.2.1 in that there is rather an ascending order of the peak value of the Von-Mises Stresses. Height analysis is presented in Fig. 4.4. However, initial assumptions can be that a taller filter is likely to have greater stresses with an increased taper angle due to an increase in the surface area on which the downward distributed loading can act on. Fig. 4.3.1(a) has a peak value of 0.778 MPa, with Fig. 4.3.1(c) having a peak of 1.162 MPa.

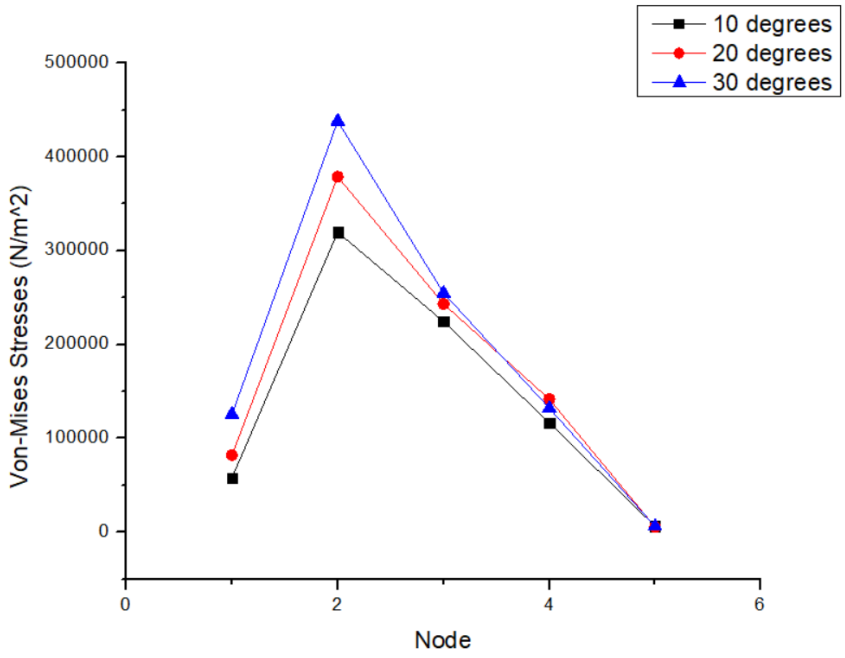

***Figure. 4.3.2**: Graph Showing Probed Von-Mises Stresses in Descending Height throughout the filter of the corresponding taper angles with a filter height of 30cm*

Fig. 4.3.1 shows that the Von-Mises stresses the filters at the height of 30cm peak at Node 2. This is an indication that this is where the stress concentrations lie on the filter. Node 2 is approximately 6 cm from the top of the filter. It is to note that possible reinforcement or having the composite material having a slightly larger thickness will ensure that the filter does not fail prematurely under a distributed load. Having identical shapes could thus mean that it will be best to use the other criteria on the Pugh Chart in Table 3.3 to determine which filter is best used.

4.1.3 Effect of Height on Stress Concentrations

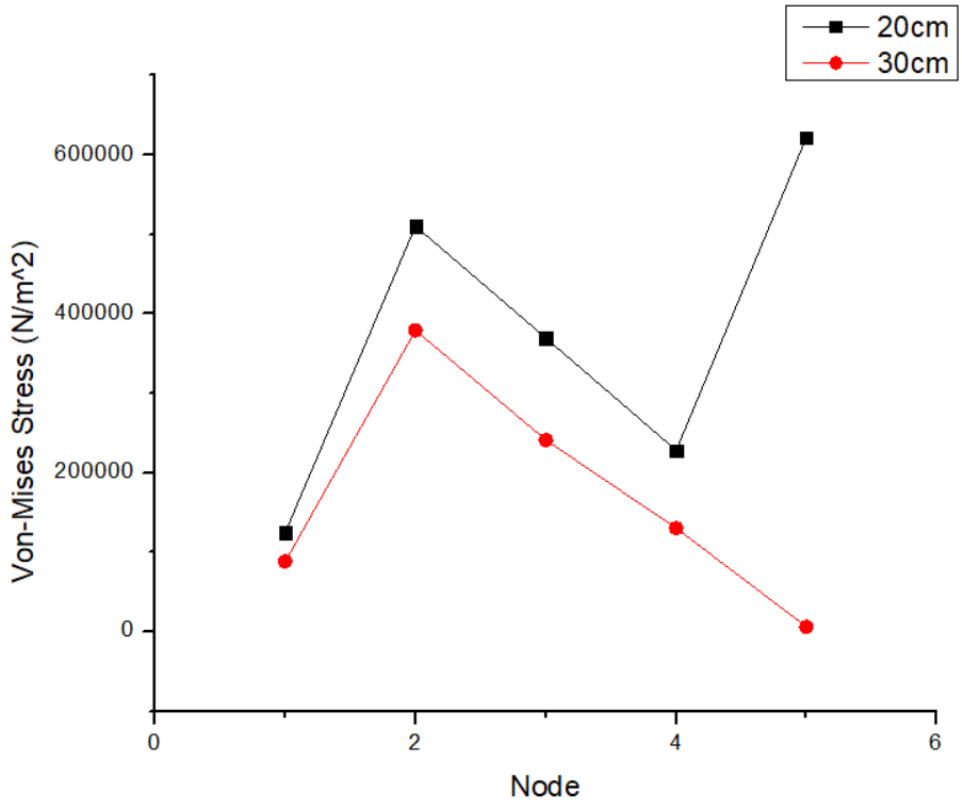

Figure. 4.4: *Graph showing average Von-Mises Stresses probed at each node for both filter heights chosen*

The graph was drawn using averages from each filter height at each probed node and plotted together on the same graph to see which had a greater stress peak. Though the trend in Fig. 4.2 and Fig. 4.3 showed an inverse relationship in the stress peaks act in the opposite direction with the two heights chosen, we see in Fig. 4.4 that there is a directly proportional relationship till it reaches node 4. Both heights peak at node 2, which is 4 cm and 6cm from the top of the 20 cm and 30 cm filters, and at 0.37 MPa and 0.5MPa, respectively. This is sharply followed by a decline down to node 4. As the 30cm filter continues down, we see another sharp increase in the stress in the 20 cm filter. With the diameter for both filters kept constant, the 30 cm filter can be said to have both a greater contact surface area and a volume. This could be why approaching the last

node at the bottom, and we see the stress for the 20cm filter rise to above 0.6 MPa and fall to almost 0 for the 30cm filter.

4.1.3. Analysis of Finalized Ceramic Filter Design

Loading analyses were done on the filter presented in Fig. 3.5 in an attempt to simulate the effect of having a full capacity for the filter.

(a)

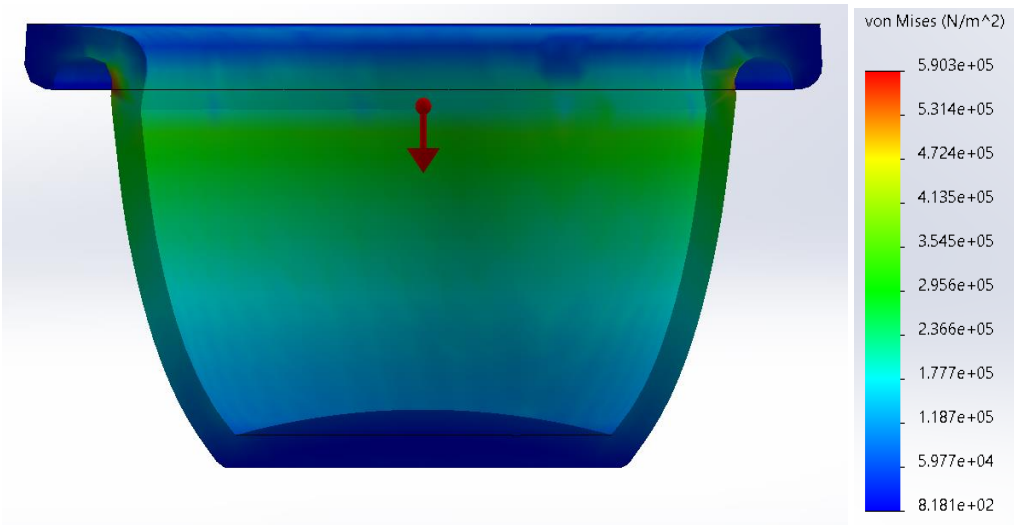

(b) (c)

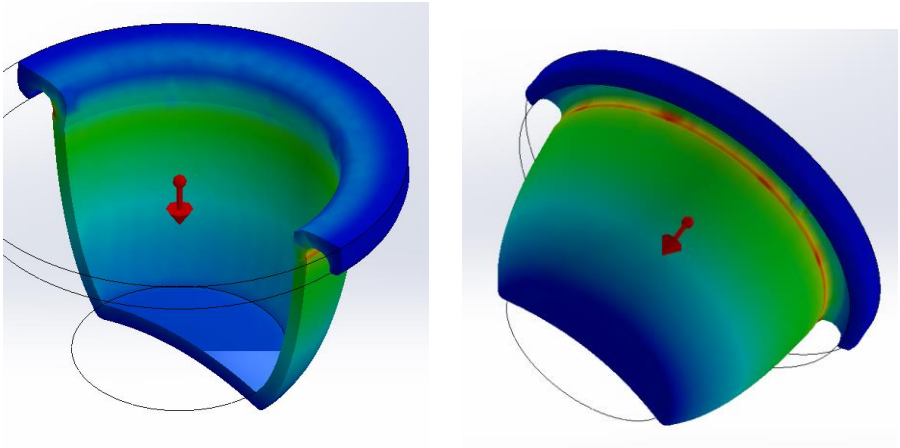

Figure 4.5.1: *3D SolidWorks Visualization of Cut Faces of Stress Distributions of Finalized Filter Design: (a) Front View, (b) Isometric View, and (c) Focus On Stress Concentration at Filter Handle Filter*

Fig. 4.5.1 shows different views of the simulation of the finalized design for the ceramic filter. Stress distribution showing relatively low Von-Mises stresses, at 0.5 MPa, even when the model is dimensionally accurate, indicating that when this filter is built, it will not be subjected to any yielding and consequently failure during the storage and usage process. This model featured a fillet of 3cm through the circumference of the bottom of the edge. This was to decrease the stress concentration factor of the overall filter leaving as there were sharp edges present at those edges. This is evident in the simulation presented in Fig. 4.5.1 (c) where there is a streak of red directly on the handle base. This is an indication of higher stress being present on those edges, hence the fillets.

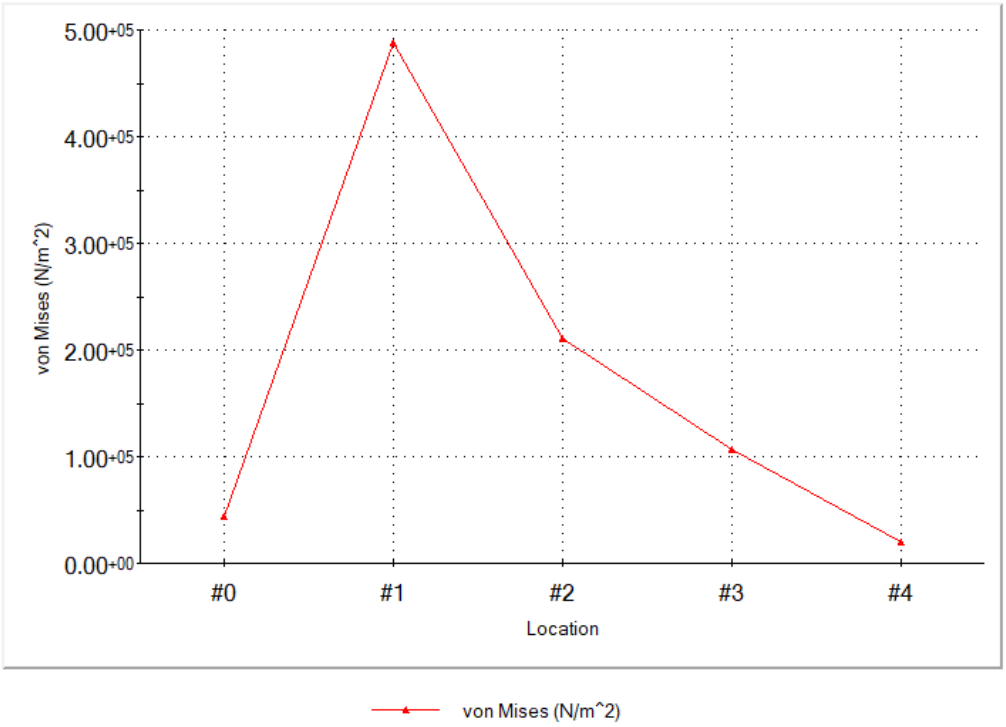

Figure. 4.5.2*: Graph Showing Probed Von-Mises Stresses in Descending Height throughout the filter of the Finalized Ceramic Filter Model*

Fig. 4.5.2 shows peak stress at node 1, approximately 4 cm from the top of the filter. This is because that node is directly beneath the handle of the filter, where the stress are concentrated due to the sharp change in geometry. Throughout the rest of the filter, the stresses are seen to decline in a rather expected motion.

(a) Displacement

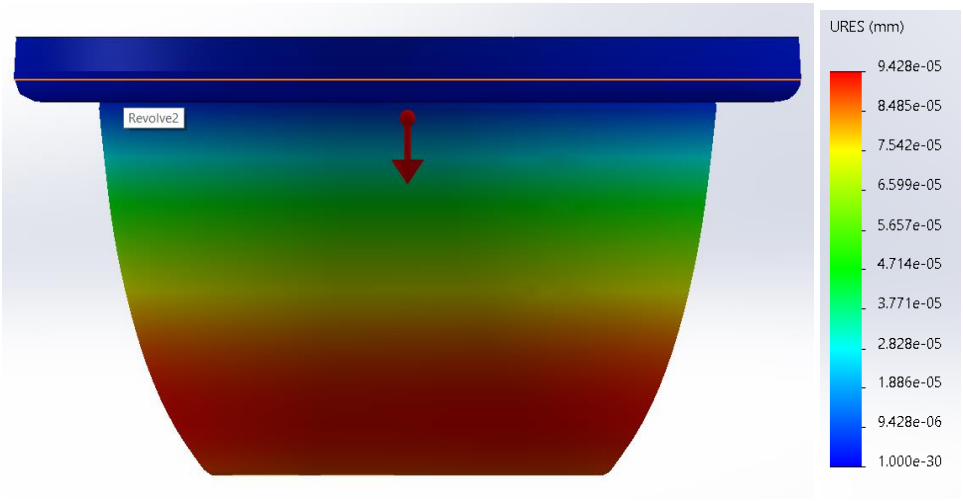

(b) Strain

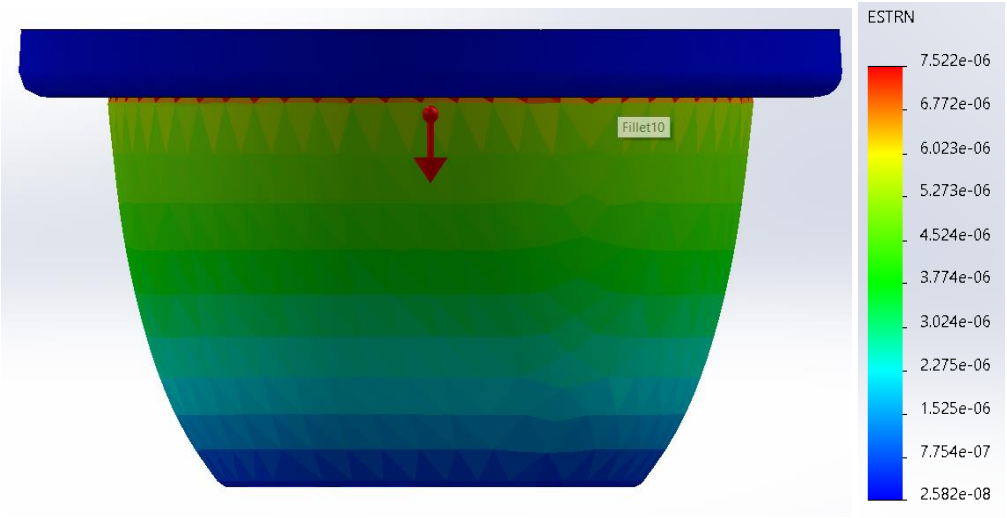

Figure 4.5.3: *3D SolidWorks Simulation Visualization of the Finalized Filter Design: (a) displacement and (b) Strain*

Fig. 4.5.3 shows the displacement and strain visualization provided by the simulation of the finalized filter design. Fig. 4.5.3 (b) showcases the directly proportional relationship between stress and strain, as there are sparsely visible streaks of red under the filter, indicating a higher level of strain directly under the handle. Fig. 4.5.3 (a) shows the uniform displacement due to the downward forces, from both gravity and the distributed loading acting downwards on the filter.

4.2 Shrinkage Testing Analysis

Dimensional differences are a direct indication of the shrinkage that the clay experiences in the drying and firing processes of the clay. The length of the clay slabs produced stood at 11cm before firing and at 10.76 cm after firing. A mechanical Vernier Caliper (tolerancing = +- 0.03mm) was used in measuring the dimensions of these slabs.

$$(\%P_L) = \left|\frac{10.46 - 11}{11} \times 100\right|$$

$$(\%P_L) = 4.909\%$$

The PFP protocol for clay testing suggests that good clay should have a shrinkage rate between 6.25 – 7.25%. However, this value is accepted for usage due to its proximity to the value. Some impurities within the clay or the manufacturing process of the slabs could be the main reason for this.

4.3 Apparent Porosity Analysis

The major dilemma in the production of ceramic filters lies in the inverse relationship between the porosity, which affects the flow rate of the filters and the strength of the filters. The porousness of the filter is created when firing occurs, and the sawdust that within it is combusted away. However, as seen in chapter 4.2, some shrinkage occurs during the firing process. Though

dimensionally minute, this greatly affects the internal porosity of the filter. This process is referred to as vitrification [44]. Using Formulas 3.3 and 3.4, the apparent porosity and the water absorption percentages were calculated for each composite slab done and recorded in Table 4.1.

Table 4.1: Table showing the apparent porosity and water absorption percentages for each composite slab done

Slab No.	Clay (%)	Sawdust (%)	Apparent Porosity (%)	Water Absorption (%)
Composite 1	40	60	63.12	68.6
Composite 2	50	50	56.60	52.32
Composite 3	60	40	49.23	42.06
Composite 4	70	30	35.67	22.18
Composite 5	80	20	37.01	23.51
Control Sample	100	0	16.24	7.79

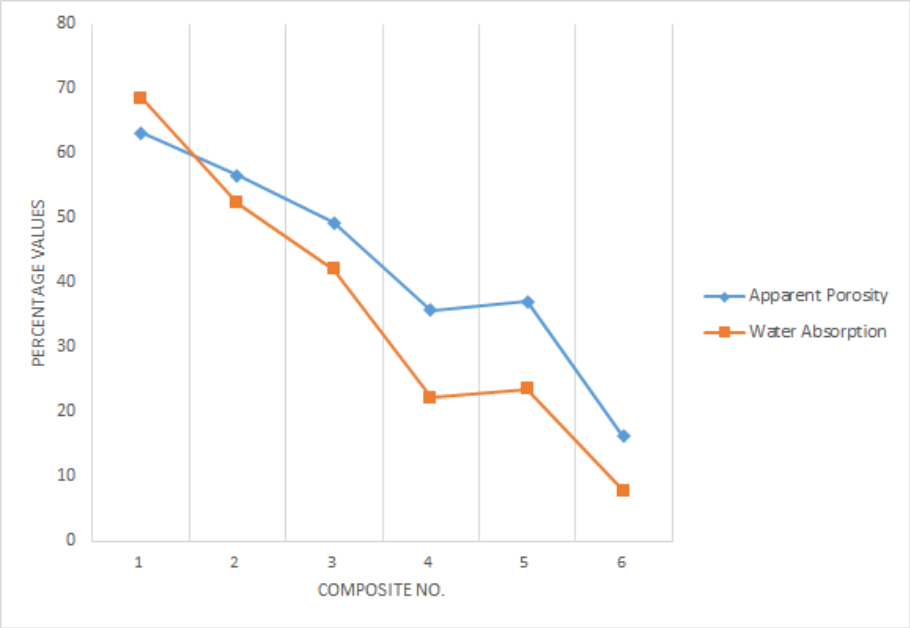

Figure 4.6: *Graph showing the trend between the apparent porosity and water absorption percentages*

From Table 4.1 and Graph 4.6, there is an evident downward trend or directly proportional relationship between the apparent porosity, water absorption, and the ratio of sawdust within the composite slab. The highest amount of sawdust fell into the 40-60% ratio, with the apparent porosity being 63.12% and the water absorption being 68.6%. The lowest amount of sawdust, bar the control used, surprisingly happened to be the composite with the 70-30 ratio, with its apparent porosity being 35.67% and water absorption being 22.18%. The control proved the notion that without the combustible material within it, there would be very little porosity, which in turn significantly decreases the flow rate for the filter with which the composition would be based on.

4.4 Impact Loading Analysis

Impact loading testing, similar to the Charpy Test, was performed to see the point of yielding and fracture for the bricks made, and the results are as seen in Table 4.2. Damage Assessment is a qualitative form that determines the extent of the damage created by the slab's point of failure and how this impacts its overall structural integrity. This value was measured on a unit step scale of 1-5, with 1 representing minute amounts of damage as a result of failure, and 5 representing great amounts of damage resulting from the failure.

Table 4.2: Table showing the number of loadings leading to failure and the corresponding damage assessment for each composite slab

Slab No.	Clay (%)	Sawdust (%)	No. Of Loadings For Failure	Damage Assessment
Control Sample	100	0	3	2
Composite 1	40	60	1	5
Composite 2	50	50	3	4
Composite 3	60	40	2	2
Composite 4	70	30	3	1
Composite 5	80	20	4	2

Table 4.2 shows the effects of the impact loading analysis on the composite slabs produced for testing. This table shows that the composite with the lowest amount of clay within it (Composite 1: 40-60 ratio) required the lowest number of continuous loadings to cause failure within it. Composite 4 had the filter with the highest number of continuous loading required to cause failure, indicating that it was the strongest of the slabs chosen.

4.5 Drop Test Analysis

The third batch of slabs was used for the qualitative drop test analysis, where slabs were each dropped from a distance of 1.3 m and were released to hit the ground and determine which one received the most damage from the fall. Much like data recorded in Table 4.2, this damage was rated on a unit step linear scale of 1-5, where damages were assessed based on intensity and crack propagation.

Results showed that composite 4-5 had the highest strength values, with ratios of 70-30 and 80-20 respectively, withstanding the drop on three different occasions. Composite 1, on the other hand, received a diagonal crack across the length cross-section of the bottom face of the brick.

4.6 Hardness Testing

All slabs were able to pass the fingernail hardness test as none of them got deformed after being scratched.

4.7 Pugh Chart for Final Compositional Choice

Table 4.3: Table showing the number of loadings leading to failure and the corresponding damage assessment for each composite slab

Slab No.	Apparent Porosity	Water Absorption	Impact Loading Test	Drop Test	Total
Control Sample	1	1	3	1	6
Composite 1	5	5	1	2	13
Composite 2	4	4	3	3	14
Composite 3	4	4	4	3	15
Composite 4	2	2	5	5	14
Composite 5	3	3	5	4	15

This Pugh Chart shows both composite 3 (ratio: 60:40) and composite 5 (ratio: 80:20) as the ideal compositional choices for producing the ceramic filter. Further analysis and discretion would be used in determining which of these, along with the ideal orientation and dimensions, to use in the finalized model for production.

Chapter 5

5.0 Conclusions & Iterations

5.1 Conclusion

The scope of this project enabled a range of tools to be used in order to achieve the most desired results of a ceramic filter that is optimized for the ideal balance between flowrate and strength. In doing so, factors like toughness, porosity and even aesthetics had to be considered. With an extensive design chapter, this research allows for options based on the specific configuration of ceramic filters required.

Results showed that using filters with height dimensions of either 20 cm with a taper angle of 10^{o} and 30cm with a taper angle of 20^{o}. The results go on to identify that in building ceramic filters, it would be best to use either a 60-40 or 80-20 ratio of clay to combustible material, which in this case was sawdust. This would ensure that the filter has an appropriate balance between strength and flowrate.

Choosing the right geometry and composition is subject to the needs of the manufacturer and the user. Some of the factors that influence the final choice include, but are not limited to, storage issues, distribution discrepancies, the quantity of water to be stored, the number of filters to be produced within a given time period, and the desired flow rate. This enables the acknowledgement that there is no concrete way of optimizing the ceramic filter for all users. However, this research allows differentiation between the best configurations for production and usage under specific conditions.

5.2 Future Recommendations

As resources were limited throughout this research project is an indication that quite a number of things could have been considered to further mechanically optimize the ceramic filters in production today.

One of the essential aspects of the production of ceramic filters is firing. Firing allows for the combustible materials to be fired away, creating the pores within the ceramic filter for water to pass through. Clay is known to react differently to a host of firing temperatures and techniques. Future works could make use of pyrometric cones to be able to tell when the slab samples have been fired to specific temperatures and the effect this has on the clay. This would enable testing to be done at specific temperatures, allowing for more accurate results. Furthermore, using a controlled firing station would be essential in controlling the rise and fall of the temperature of the clay. This would enable for a smoother curing process and allow for water to appropriately evaporate out and the material to combust evenly.

Another aspect that could be investigated could be using a host of other materials, specifically different types of clay sourced from different regions. This would enable one to identify which clay works best under certain loading and flow conditions and specific environments. Furthermore, this would allow for testing to be done on the different strengths of the clays to see which ones are structurally superior and which to be avoided at all costs in the production of ceramic filters. Moreover, the use of different combustion materials in the data collection process would allow for the determining of which particles and microbes can pass through the filter, hence improving or decreasing its efficacy.

5.3 Limitations

Being in uncertain times like these led to several challenges being encountered throughout the workings of this project. The ever-looming presence of Covid-19 causing many laboratories and factories to be either closed or operating with limited functionality meant that the intended outcome and scope has to be iterated on three different occasions. Sourcing clay was the major challenge because many factories were either out of reach or unwilling to sell the already scarce clay at exorbitant prices. Sawdust, on the other hand, was relatively easier to acquire. The production of a kiln for firing was another major challenge. This was due to the fact that it was seen as a major safety hazard, operating such high temperatures without the appropriate tools to control the flame in a residential setting, handling the equipment required to take the samples out of the fire and the lack of PPE required to indulge in any flame-related activity.

References

[1] UNEP (2020). Tackling global water pollution. Retrieved from https://www.unep.org/explore-topics/water/what-we-do/tackling-global-water-pollution

[2] Rethman, M. (2019, December 16). 8 Facts About Ghana's Water Crisis. Retrieved from https://borgenproject.org/8-facts-about-ghanas-water-crisis/

[3] WaterAid US. (n.d.). Ghana: WaterAid US. Retrieved February 2, 2021, from https://www.wateraid.org/us/where-we-work/ghana

[4] UNICEF Data. (2020, October 27). Diarrhoea. Retrieved January 24, 2021, from https://data.unicef.org/topic/child-health/diarrhoeal-disease/

[5] World Health Organization. (2019, June 14). Drinking-water - Fact Sheet. Retrieved January 23, 2021, from https://www.who.int/news-room/fact-sheets/detail/drinking-water

[6] World Life Expectancy. (2018). Diarrhoeal diseases in Ghana. Retrieved January 24, 2021, from https://www.worldlifeexpectancy.com/ghana-diarrhoeal-diseases

[7] Adjei, A. A., Armah, H., Rodrigues, O., Renner, L., Borketey, P., Ayeh-Kumi, P., ... & Lartey, M. (2004). Cryptosporidium spp., a frequent cause of diarrhea among children at the Korle-Bu Teaching Hospital, Accra, Ghana. Japanese journal of infectious diseases, 57(5), 216-219.

[8] Ahmad, R. (2005). Particulate Matter Removal by Filtration and Sedimentation. Water Encyclopedia. doi:10.1002/047147844x.mw406

[9] Wong, J. M. (1984). Chlorination-Filtration for Iron and Manganese Removal. Journal - American Water Works Association, 76(1), 76-79. doi:10.1002/j.1551-8833.1984.tb05265.x

[10] Cost-effective aeration. (2015). Filtration Separation, 52(6), 12. doi:10.1016/s0015-1882(15)30253-6

[11] AO Smith India. (2019, July 23). Easy and Effective Ways to Purify Water. Retrieved January 5, 2021, from https://www.aosmithindia.com/blog/easy-and-effective-ways-purify-water

[12] Conradie, E. M. (2018). To Cover the Many Sins of Galamsey Mining. Missionalia, 46(1). doi:10.7832/46-1-274

[13] Tchounwou, P. B., Yedjou, C. G., Patlolla, A. K. and Sutton, D. J. Heavy Metals Toxicity, and the Environment. *EXS*, *101* (2012) 133-164. https://doi.org/10.1007/978-3-7643-8340-4_6.

[14] Study Session 10 Household Water Collection, Treatment, Storage and Handling. (n.d.). Retrieved from https://www.open.edu/openlearncreate/mod/oucontent/view.php?id=80352§ion

[15] World Health Organization. (2019, June 14). Drinking-water - Fact Sheet. Retrieved January 23, 2021, from https://www.who.int/news-room/fact-sheets/detail/drinking-water

[16] Centers for Disease Control and Prevention. (2019). Cholera. Retrieved December 13, 2020 from http://www.cdc.gov/cholera/index.html.

[17] WHO. (2017, September 18). Number of reported cholera cases. Retrieved from https://www.who.int/gho/epidemic_diseases/cholera/cases_text/en/

[18] Mubarik, A. (2017, May 13). 60% of Ghana's water bodies polluted – Water Resources Commission. Retrieved from https://www.business-humanrights.org/fr/dernières-actualités/ghana-60-of-water-bodies-polluted-due-to-illegal-mining-and-other-activities-say-authorities/

[19] Kani, M.K. and Nair, C. (2017). Effectiveness of Locally Made Ceramic Water Filters for Household Water Purification. 7. 75-82.

[20] Ajayi, B. and Lamidi, Y. (2015) Formulation of Ceramic Water Filter Composition for the Treatment of Heavy Metals and Correction of Physiochemical Parameters in Household Water. Art and Design Review, 3, 94-100. doi: 10.4236/adr.2015.34013.

[21] Kresh, M. (2018, October 15). How Clay Jugs Make Polluted Water Safe. Retrieved from https://www.greenprophet.com/2018/10/how-clay-jugs-make-polluted-water-safe/

[22] Woodford, C. (2021). What are ceramics?. Retrieved 21 March 2021, from https://www.sciencelearn.org.nz/resources/1769-what-are-ceramics

[23] Science Learning Hub – Pokapū Akoranga Pūtaiao. (2021). What are ceramics?. Retrieved 10 March 2021, from https://www.sciencelearn.org.nz/resources/1769-what-are-ceramics

[24] Foley, N. K. (1999, September). Environmental Characteristics of Clays and Clay Mineral Deposits. Retrieved from https://pubs.usgs.gov/info/clays/

[25] CDC. (2011, June). Best Practice Recommendations for Local Manufacturing of Ceramic Pot Filters. *1*. Retrieved from https://b06e35ce-2a1a-4f6b-935c-3a97c8f0fbb7.filesusr.com/ugd/2802c0_91b40a48e8a348e5989aa91b6d2d8998.pdf

[26] Swanton, A. A. (2008). Evaluation of the complementary use of the ceramic (Kosim) filter and Aquatabs in northern region, Ghana (Unpublished doctoral dissertation). Massachusetts Institute of Technology, Dept. of Civil and Environmental Engineering

[27] Callister, W. D., & Rethwisch, D. G. (2020). Materials science and engineering. Hoboken, NJ: Wiley.

[28] LL Special Furnace Co. (2020, February 25). What are Ceramic Matrix Composites? Retrieved from https://llfurnace.com/blog/what-are-ceramic-matrix-composites/

[29] Krenkel, W., & Reichert, F. (2018). 5.1 Design Objectives and Design Philosophies, Interphases and Interfaces in Fiber-Reinforced CMCs. *Comprehensive Composite Materials II*, *5*, 1-18. doi:10.1016/b978-0-12-803581-8.09986-0

[30] Phonphuak, N., & Chindaprasirt, P. (2015). *Eco-Efficient Masonry Bricks and Blocks*. doi:10.1016/B978-1-78242-305-8.00006-1

[31] Proto, A. R., Zimblatti, G., & Negri, M. (2010). The Measurement & Distribution of Wood Dust. *Journal of Agricultural Engineering*, *1*, 25-31.

[32] Potters for Peace (PFP). (2008). Accessed 12 February 2021.

[33] Zereffa, E. A. & Bekalo, T. (2017). Clay Ceramic Filter for Water Treatment. Materials Science and Applied Chemistry. 34. 10.1515/msac-2017-0011.

[34] van Halem, D. (2006) Ceramic silver impregnated pot filters for household drinking water treatment in developing countries. Unpublished Thesis, Delft University of Technology, Delft.

[35] Lantagne, D.S. (2001) Investigation of the Potters for Peace Colloidal Silver Impregnated Ceramic Filter Report 1: Intrinsic Effectiveness. Alethia Environmental: Allston, MA, USA.

[36] Peterson, B. (2020, July 8). How Temperature Changes Clay. Retrieved from https://www.thesprucecrafts.com/how-temperature-changes-clay-2746240

[37] Pelita (2009). Indonesia (Indo-2): Photograph provided by Pelita Indonesia in response to questionnaire.

[38] Kulinkina, A. V., Kosinski, K. C., Liss, A., Adjei, M. N., Ayamgah, G. A., Webb, P., Gute, D. M., Plummer, J. D., & Naumova, E. N. (2016). Piped water consumption in Ghana: A case study of temporal and spatial patterns of clean water demand relative to alternative water sources in rural small towns. *The Science of the total environment*, *559*, 291–301. https://doi.org/10.1016/j.scitotenv.2016.03.148

[39] Ghana, Ghana Statistical Service. (2013). *2010 Population & Housing Census Report*.

[40] Gieck, K., & Gieck, R. (2014). Engineering formulas. Brantford, Ontario: W. Ross MacDonald School Resource Services Library.

[41] Beer, F. P., DeWolf, J. T., Johnston, E. R., & Mazurek, D. F. (2020). *Mechanics of materials*. New York, NY: McGraw-Hill Education.

[42] Amazian, L. (2018, November). Unfired Clay Bricks with Enhanced Properties Project Report [Scholarly project]. In Al Akhawayn University School Of Science & Engineering. Retrieved from http://www.aui.ma/sse-capstone-repository/pdf/fall-2018/Unfired Clay Bricks with Enhanced Properties.pdf

[43] ASTM, C. Standard test method for water absorption, bulk density, apparent porosity, and apparent specific gravity of fired whiteware products. West Conshohocken, Pennsylvania, US: ASTM International. (2006) C373-88.

[44] van Halem, D. (2006) Ceramic silver impregnated pot filters for household drinking water treatment in developing countries. Unpublished Thesis, Delft University of Technology, Delft